

TEXAS
TRANSPORTATION
INSTITUTE

TEXAS
HIGHWAY
DEPARTMENT

COOPERATIVE
RESEARCH

SOIL DAMPING CONSTANTS RELATED
TO COMMON SOIL PROPERTIES
IN SANDS AND CLAYS

in cooperation with the
Department of Transportation
Federal Highway Administration
Bureau of Public Roads

RESEARCH REPORT 125-1

STUDY 2-5-67-125

BEARING CAPACITY FOR AXIALLY LOADED PILES

**SOIL DAMPING CONSTANTS RELATED TO COMMON
SOIL PROPERTIES IN SANDS AND CLAYS**

by

Gary C. Gibson

Research Assistant

and

Harry M. Coyle

Associate Research Engineer

Research Report Number 125-1

Bearing Capacity for Axially Loaded Piles

Research Study Number 2-5-67-125

Sponsored by

The Texas Highway Department

In Cooperation with the

U. S. Department of Transportation,

Federal Highway Administration,

Bureau of Public Roads

September 1968

**TEXAS TRANSPORTATION INSTITUTE
Texas A&M University
College Station, Texas**

Preface

The information contained herein was developed on Research Study 2-5-67-125 entitled "Bearing Capacity for Axially Loaded Piles" which is a cooperative research study sponsored jointly by the Texas Highway Department and the U. S. Department of Transportation, Federal Highway Administration, Bureau of Public Roads. The broad objective of this project is to develop a procedure whereby the bearing capacity of an axially loaded pile can be determined for any combination of soil and driving conditions.

This is the first research report on this study. The report presents the results of a laboratory investigation of the damping properties of sands and clays. An effort was made in this investigation to relate these damping properties to other common properties of the soils tested.

A series of dynamic (impact) and static tests were performed on a variety of sands and clays. The sands varied in grain size and grain shape, and the clays varied in plasticity and moisture content. Velocity of sample deformation, peak dynamic loads, and peak static loads were measured so that damping constants for the soils could be evaluated.

A mathematical model in current use which describes soil action at the point of a pile was examined. A modification of this model was made in order to achieve a constant damping value over the full range of loading velocities. The damping constant is related to void ratio and effective angle of internal shearing resistance in sands and moisture content and liquidity index in clays.

It should be noted that the phase of the research covered in this report had the limited objective of establishing which soil properties could be correlated with the damping characteristics of the soils tested. It is not known at this time whether the damping constants obtained in this study from laboratory tests can be used in wave equation analysis of piling behavior or for estimation of pile bearing capacity. Subsequent reports will present damping constants obtained from small scale field tests and should have direct application for use in wave equation analysis.

The opinions, findings, and conclusions expressed in this report are those of the authors and not necessarily those of the Bureau of Public Roads.

TABLE OF CONTENTS

LIST OF TABLES.....	iv
LIST OF FIGURES.....	v
CHAPTER	Page
I. INTRODUCTION.....	1
Study of dynamic behavior of piling.....	1
Study of dynamic behavior of soils.....	2
Scope of this study.....	2
Objectives of this study.....	2
II. APPARATUS, INSTRUMENTATION, AND TEST PROCEDURE.....	2
General.....	2
Triaxial cells.....	2
Loading system.....	3
Force, displacement, and pore pressure measurement.....	4
Recording system.....	4
Calibration of equipment.....	4
Test procedure.....	4
III. RESULTS OF TESTS ON SANDS.....	5
General.....	5
Determination of a constant damping value.....	6
Summary of results.....	9
IV. RESULTS OF TESTS ON CLAYS.....	9
General.....	9
Determination of a constant damping value.....	10
Damping constant related to certain clay properties.....	13
Summary of results.....	16
V. CONCLUSIONS.....	16
VI. RECOMMENDATIONS.....	16
LIST OF REFERENCES.....	17
APPENDIX A—Data Reduction from the Visicorder Trace.....	18
APPENDIX B—Explanation of Computer Program to Determine Damping Constant.....	19
APPENDIX C—Determination of Optimum Power for Velocity of Deformation.....	25
APPENDIX D—Mohr's Circle Diagrams for the Granular Materials Tested.....	26

LIST OF TABLES

Table	Page
I. Results of Tests on Ottawa Sand.....	7
II. Results of Tests on Arkansas Sand.....	7
III. Results of Tests on Victoria Sand.....	7
IV. Error Resulting from Approximations.....	8
V. Study of Void Ratio Change in Ottawa Sand.....	9
VI. Results of Tests on OR31 Clay.....	11
VII. Results of Tests on OR36 Clay.....	12
VIII. Results of Tests on OR37 Clay and Study of Effect of Confining Pressure.....	12
IX. Results of Tests on EA62 Clay.....	12
X. Results of Tests on EA60 Clay.....	12
XI. Results of Tests on EA55 Clay.....	13
XII. Results of Tests on EA50 Clay.....	13
XIII. Results of Tests on VE55 Clay.....	14
XIV. Results of Tests on VE50 Clay.....	14
XV. Results of Tests on VE46 Clay.....	14
XVI. Results of Tests on Hall Pit Sandy-Clay.....	15
XVII. Error Resulting from Approximations Results of J Values for $N = 0.18$	15

LIST OF FIGURES

Figure	Page
1 Soil Resistance versus Deformation Diagram for Soils.....	1
2 Smith's Rheological Model (after Smith).....	1
3 Picture of Apparatus and General Schematic Diagram of Setup.....	3
4 The Triaxial Base Load Cell.....	3
5 Loading Apparatus.....	3
6 Average Velocity of Deformation versus Height of Drop.....	4
7 Grain Size Curve for Sands Tested.....	5
8 Equipment setup for Impact Test on Ottawa Sand.....	5
9 Velocity of Sample Deformation versus Peak Dynamic Load for Sands Tested.....	6
10 $P_{dynamic}/P_{static}$ versus Velocity of Deformation for Sands Tested.....	6
11 Smith's J versus Velocity of Deformation for Sands Tested.....	6
12 Damping Constant versus Velocity for Deformation Raised to Optimum Power for Sands Tested.....	7
13 Damping Constant versus Velocity of Deformation Raised to .20 Power for Sands Tested.....	8
14 Effective Angle of Internal Shearing Resistance versus Damping Constant for Sands Tested.....	8
15 Peak Dynamic Load versus Velocity of Deformation for Void Ratio Study on Ottawa Sand.....	8
16 Void Ratio versus Damping Constant for Ottawa Sand.....	9
17 Location on Plasticity Chart of Clays Tested.....	10
18 Vettors Clay at Three Moisture Contents Before and After Failure.....	10
19 Effect of Confining Pressure on OR 37 Material.....	10
20 Effect of Sample Height on Dynamic Load in OR 36 Material.....	10
21 Dynamic Load versus Velocity of Deformation for Clays Tested.....	11
22 Ratio of Dynamic to Static Load versus Velocity of Deformation for Clays Tested.....	11
23 Smith's J versus Velocity of Deformation for EA 50 Material.....	11
24 Damping Constant at $N = \text{Optimum}$ versus Velocity of Deformation for Clays.....	13
25 Damping Constant at $N = 0.18$ versus Velocity of Deformation for Clays Tested.....	13
26 Moisture Content versus Damping Constant for Vettors Clay.....	14
27 Liquidity Index versus Damping Constant for Clays Tested.....	15
A-1 Sample Visicorder Trace.....	18
C-1 Method of Obtaining Velocity to Optimum Power.....	25
D-1 Mohr's Circle Diagram for Ottawa Sand.....	26
D-2 Mohr's Circle Diagram for Arkansas Sand.....	27
D-3 Mohr's Circle Diagram for Victoria Sand.....	28

NOTATION

The following symbols are used in this study:

c	= a viscous damping constant,	OR 37	= organic material at an approximate moisture content of 37 percent,
CE 35	= Hall Pit sandy clay at an approximate moisture content of 35 percent,	$P_{dynamic}, P_d$	= dynamic strength of soil, pounds,
e	= void ratio,	P_{static}, P_s	= static strength of soil, pounds,
EA 62	= Easterwood clay at an approximate moisture content of 62 percent,	psi	= pounds per square inch,
EA 60	= Easterwood clay at an approximate moisture content of 60 percent,	Q	= maximum elastic ground deformation, inches,
EA 55	= Easterwood clay at an approximate moisture content of 55 percent,	R_u	= total ultimate plastic ground resistance, pounds,
EA 50	= Easterwood clay at an approximate moisture content of 50 percent,	R_r	= resisting force of the soil in the elastic region, pounds,
fps	= feet per second,	S	= permanent set of the soil, inches,
ft	= foot or feet,	x	= elastic deformation of the soil, inches,
in	= inch or inches,	VE 55	= Veters clay at an approximate moisture content of 55 percent,
ips	= inches per second,	VE 50	= Veters clay at an approximate moisture content of 50 percent,
J	= a viscous damping constant for soil, seconds per foot,	VE 46	= Veters clay at an approximate moisture content of 46 percent,
K'	= a spring constant for soil mass segment, pounds per inch	σ_3	= chamber pressure or confining pressure, psi
lb	= pound or pounds,	$\bar{\sigma}_3$	= effective confining pressure, psi
N	= a power to which velocity of sample deformation is raised,	ϕ	= angle of internal shearing resistance, degrees
OR 31	= organic material at an approximate moisture content of 31 percent.	ϕ'	= effective angle of internal shearing resistance, degrees.
OR 36	= organic material at an approximate moisture content of 36 percent,		

Soil Damping Constants Related to Common Soil Properties in Sands and Clays

CHAPTER I INTRODUCTION

Study of Dynamic Behavior of Piling

The dynamic behavior of piling has been of great concern to Civil Engineers for many years. In 1962, E. A. L. Smith (10)* suggested a numerical solution to the pile driving problem. Smith presented the concept for static loading at the point of a pile such that the ground compresses elastically for a certain distance and then fails plastically with a constant resistance. This concept is illustrated in Figure 1 by the dotted line OABC. Q in the figure represents the maximum elastic ground deformation or "quake" and R_u represents the total ultimate plastic ground resistance to the pile. Under static loading the pile deforms the ground elastically through OA and then plastically through a distance S . The soil then rebounds from B to C leaving a permanent set of S .

E. A. L. Smith (10) developed a mathematical model which accounts for both static and dynamic soil behavior. Figure 2 shows the rheological model which simulates the mathematical model proposed by Smith. The model consists of a spring and friction block in series connected in parallel to a dashpot. If the model were suddenly compressed a certain distance, the following equation would describe the soil's resistance in the elastic region (see Figure 1):

*Numerals in parentheses refer to corresponding items in list of references. The citations on the following pages follow the style of the *Journal of the Soil Mechanics and Foundations Division, American Society of Civil Engineers*.

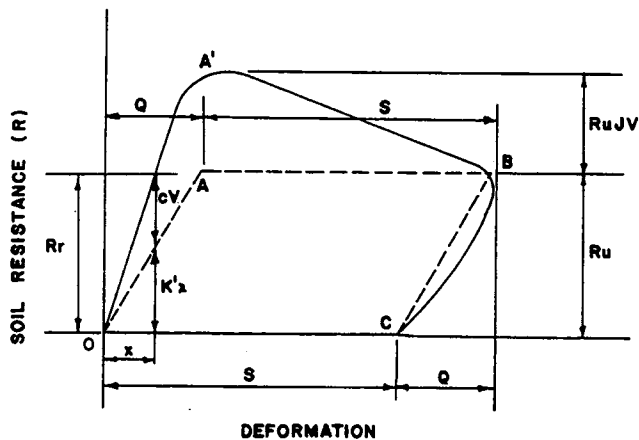


Figure 1. Soil resistance versus deformation diagram for soils.

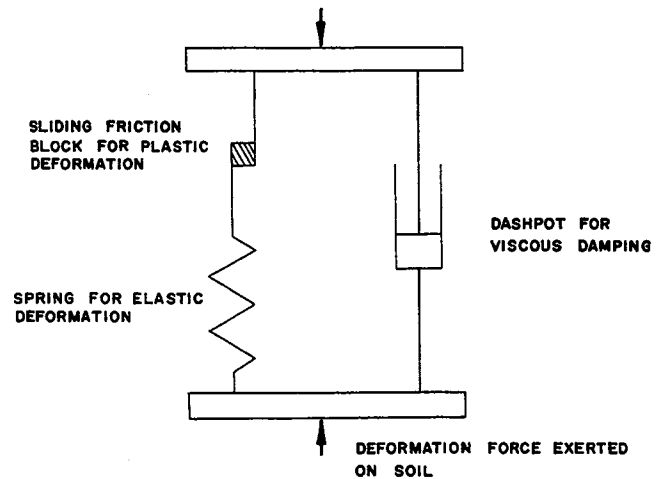


Figure 2. Smith's rheological model (after Smith).

$$R_r = K'x + cV \quad (1)$$

where:

- R_r = resisting force,
- K' = soil spring constant,
- c = a viscous damping constant,
- x = elastic deformation of the soil or "Quake,"
- V = the instantaneous velocity of the point of the pile in any time interval.

The friction block accounts for the constant soil resistance in the plastic region during static loading and thus does not appear in equation 1. In order to include the effect of the pile's size and shape Smith has made:

$$c = K'xJ \quad (2)$$

where J is a viscous damping constant for the soil similar to c . As the velocity of deformation approaches zero in equation 1, the dynamic resisting force approaches a static value:

$$P_{static} = K'x \quad (3)$$

Letting $P_{dynamic}$ equal R_r in equation 1 from Smith's mathematical model and substituting equations 2 and 3 into 1, the peak dynamic resistance of the soil is:

$$P_{dynamic} = P_{static} (1 + JV) \quad (4)$$

Samson, Hirsch and Lowery (7, 8) expanded Smith's static loading concept to the dynamic concept represented by line OA'BC of Figure 1. If R_u in Figure 1 is the static soil resistance, then $R_u JV$ is the dynamic portion of the total soil resistance.

This concept for the resistance at the point of the pile takes into account:

1. elastic ground deformation,
2. ultimate ground resistance, and
3. viscous damping constant based on damping constant "J".

Smith assigned a value of $J = 0.15$ for use by investigators until such time that new facts were developed. He pointed out that his mathematical model could be modified to account for the new facts as they were obtained.

Smith's work was augmented by Samson, Hirsch, and Lowery (7, 8) so that the driving of a pile could be simulated by use of the digital computer. It was their feeling that the resistance to dynamic loading at the point of the pile is not clearly understood and that future study might shed more light on the problem.

Study of Dynamic Behavior of Soils

It is known that the compressive strength of a soil is a function of the time required to reach a failure load. Nishida (4) in his paper entitled "A Soil Strength Subject to Falling Impact" studied this effect and found it to be true. Hampton and Yoder (2) found that in silty clay and clay the unconfined compressive strength showed significant increases with rate of strain for all compactive efforts and all moisture contents tested. Whitman and Healy (12) did an extensive study on shear strength in sands during rapid loading. They developed techniques for applying strains rapidly and measuring resultant stresses and pore pressures and presented information concerning membrane and inertia effects in triaxial tests. Jones, Lister, and Thrower (3) in a related study presented a comprehensive literature study of the subject of dynamic loading of soils.

Chan (1) investigated in the laboratory the dynamic load deformation and damping properties in sands. Reeves (5) did laboratory research and evaluated the damping constants of sands subjected to impact loads.

Using experimental data and Smith's equation, Reeves determined that the damping constant, J , was actually a variable for a saturated sand. By modifying Smith's equation in the following manner he was able to obtain a constant J value.

$$P_{\text{dynamic}} = P_{\text{static}} (I + JV) \quad (5)$$

This modification of Smith's equation involves an intercept value, I . To evaluate this intercept, Reeves performed dynamic tests, finding the ratio of dynamic to static load versus velocity of sample deformation to be a straight line between velocities of 3-12 fps. He then extended this straight line to the P_a/P_s axis and obtained an intercept, I . Using this intercept in equation 5 he was able to evaluate a constant J value in the range of 3-12 fps.

Sulaiman (11) did a study in which he was concerned with the static side friction values encountered in various types of sand. Raba (6) investigated side frictional damping (J') developed in clays using a model pile in the laboratory. Raba was able to relate J' to liquidity index for CH materials.

Scope of This Study

From the foregoing discussion, it can be seen that some work has been done on pile-soil systems and evaluating damping constants for soils. With the exception of Raba's work in clays, there has been little done in relating soil damping constants to common soil properties.

Objectives of This Study

The objectives of this investigation are:

1. To determine soil damping constants for sands and clays by conducting laboratory impact tests on these soils, and
2. To correlate these soil damping constants with common soil properties such as void ratio and angle of internal shearing resistance in sands and liquidity index and moisture content in clays.

CHAPTER II

APPARATUS, INSTRUMENTATION, AND TEST PROCEDURE

General

The equipment involved in this series of tests was necessarily of a special nature. In the dynamic tests it was desired to load the sample over a range of velocities from 0-12 feet per second. It was also important that a permanent record of each test be available from which the necessary calculations could be made. Figure 3 is a picture of the complete test set-up including the dynamic loading apparatus, the triaxial cell and the recording equipment. The numbers in parentheses in Figure 3 represent the location of specific items of equipment. This figure also shows a general schematic diagram of the complete apparatus in sequence of occurrence from left to right. Only general descriptions of the

equipment are given in this chapter. Detailed information can be found in a paper by Reeves (5).

Triaxial Cells

Two separated triaxial devices with load cells in the base were used in this investigation. Figure 4 shows the cell bases used for both the cohesive and granular materials. The load cells consisted of SR-4 strain gages mounted on the walls of an aluminum tube or pedestal to record the compressional load on impact. The cell shown in Figure 4a was developed by Reeves (5) and was used in tests on sands in this study. It has provisions for drainage of the sample at both top and bottom. All sand samples were 2.8 inches in diameter and 6

ITERATION NUMBER	J-VALUE	N	TEST NO.	MATERIAL
6	1.051	0.140	110	EA50
1	0.969	0.150	115	EA50
2	0.953	0.150	114	EA50
3	0.919	0.150	113	EA50
4	0.982	0.150	112	EA50
5	1.030	0.150	111	EA50
6	1.026	0.150	110	EA50
1	0.969	0.160	115	EA50
2	0.943	0.160	114	EA50
3	0.906	0.160	113	EA50
4	0.966	0.160	112	EA50
5	1.008	0.160	111	EA50
6	1.003	0.160	110	EA50
1	0.969	0.170	115	EA50
2	0.933	0.170	114	EA50
3	0.892	0.170	113	EA50
4	0.949	0.170	112	EA50
5	0.986	0.170	111	EA50
6	0.980	0.170	110	EA50
1	0.969	0.180	115	EA50
2	0.923	0.180	114	EA50
3	0.879	0.180	113	EA50
4	0.933	0.180	112	EA50
5	0.954	0.180	111	EA50
6	0.957	0.180	110	EA50
1	0.969	0.190	115	EA50
2	0.913	0.190	114	EA50
3	0.866	0.190	113	EA50
4	0.918	0.190	112	EA50
5	0.943	0.190	111	EA50
6	0.935	0.190	110	EA50

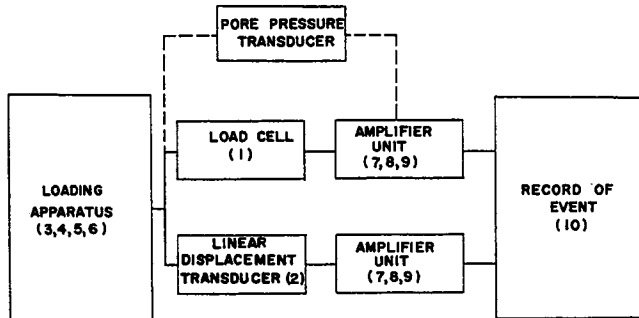
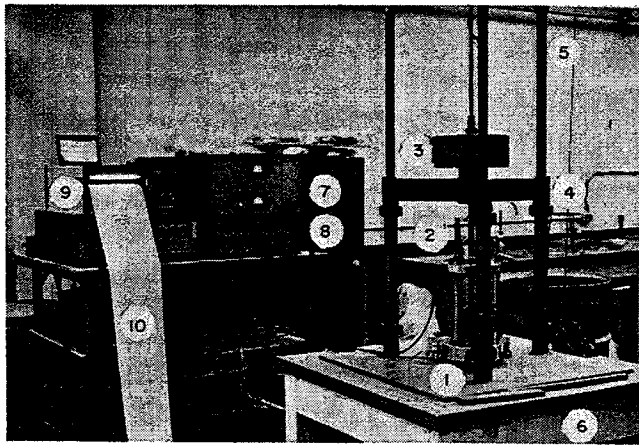


Figure 3. Picture of apparatus and general schematic diagram of set-up.

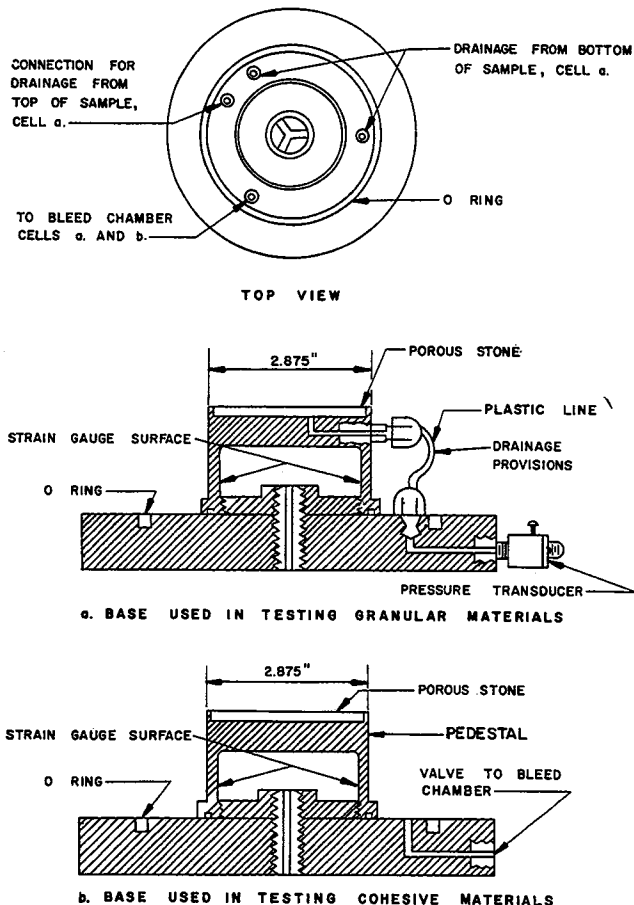


Figure 4. The triaxial base load cell.

inches long, resting on porous stones at the top and bottom. In these tests the sands were saturated and confined by air pressure in the cell which remained constant during the test. The load cell shown in Figure 4b was developed by Chan (1) and was used in tests on cohesive soil in this study. The cell has no provisions for drainage but it was more sensitive to the smaller loads recorded in cohesive materials. The cohesive specimens used in dynamic tests were 2.8 inches in diameter and $3\frac{1}{4}$ inches high. The $3\frac{1}{4}$ -inch high sample was used because there were a limited number of remolded samples available for this study and because a preliminary study was performed indicating the short sample would not affect the test results. The results of this preliminary study will be shown in Chapter IV. The cohesive static test specimens were 2.8 inches in diameter and 6 inches high.

Loading System

The loading apparatus was designed and built by Reeves (5) for use in his work on impact loading of sands. Figure 5 shows the loading apparatus and its essential parts. The falling weight of 165 pounds was sufficient to fail any sample tested given sufficient height of drop. The drop height could be varied from zero (weight resting on plunger of triaxial device) to 12 inches. In dense sands this weight was not sufficiently large to fail the sample when the weight rested on the triaxial cell's plunger, thus in these materials minimum drop heights on the order of one inch were used. The frame to stop the falling weight shown in Figure 5 could

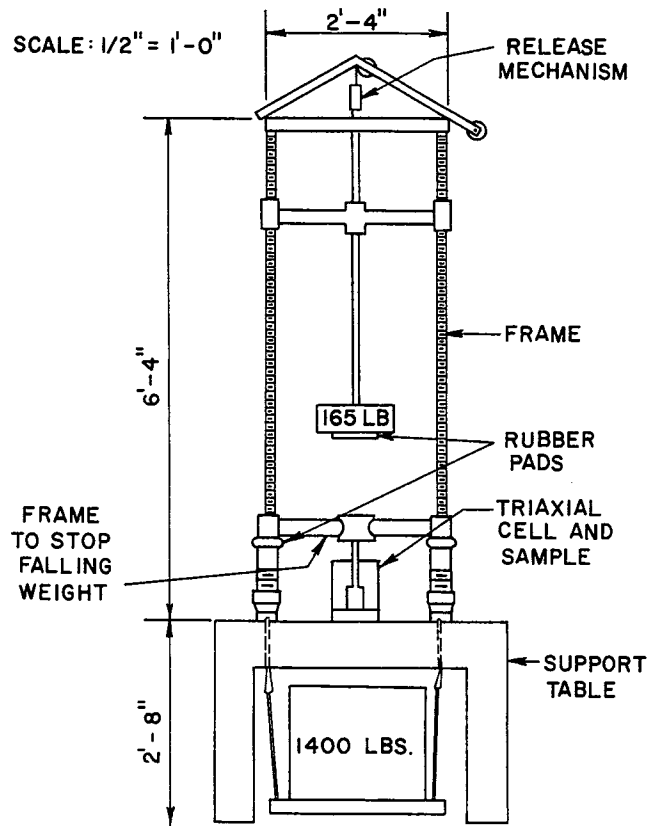


Figure 5. Loading apparatus.

be placed at a height to allow failure of a 6-inch sand sample or could be adjusted to accommodate the shorter 3 $\frac{1}{4}$ -inch samples of cohesive material. The release mechanism allowed the weight to be released instantaneously and to fall freely to impact with the plunger of the triaxial apparatus. The whole frame rested on a steel plate from which was hung 1400 pounds to damp vibrations. The rubber damping pads indicated in Figure 5 also served this purpose. The falling ram was damped by a $\frac{1}{4}$ -inch rubber pad to prevent steel-on-steel impact which caused disturbance in the recording system. The velocity of deformation of the sample could be controlled by varying the height of drop. Figure 6 shows a relationship between height of drop and average recorded displacement velocity. It should be noted that this recorded displacement velocity is higher than the velocity calculated for free falling bodies at the heights shown. The reason for this is that the large ram impacts the triaxial plunger causing it to rebound at a velocity greater than the impact velocity. This could be reduced somewhat by putting a thicker rubber pad on the ram. As can be seen from Figure 6, a range of velocities varying from 0-12 feet per second could be obtained.

The static tests were accomplished on a Soiltest, Inc. model AP-322-X compression machine and a Soiltest, Inc. model AP-170-A compression machine both run at a loading rate of 0.05 inches per minute. These tests were standard compression tests.

Force, Displacement, and Pore Pressure Measurement

Measurement of loads for the dynamic tests was accomplished by the load cells shown in Figure 4 and in the static tests loads were measured by Soiltest standard proving rings. Displacement measurements for the dynamic tests were made by means of a linear displacement transducer Model 7DCDT-1000 manufactured by Sanborn Company. As seen in Figure 3 the displacement transducer is fastened to the triaxial cell and connected to the triaxial plunger, measuring its movement. Displacement measurements for the static-triaxial tests were made with an Ames dial. Pore pressure measurements for the granular materials were made by means of a pore pressure transducer type 4-312-0001, manufactured by Consolidated Electrodynamic Corporation. Pore pressures were measured from the bottom of the sample and were recorded in only a few "pilot" tests.

Recording System

All signals from the pore pressure transducer or load cells were channeled into a Honeywell Carrier amplifier model 119 and Honeywell Visicorder Oscillograph model 1508, as seen in Figure 3. The signal from the linear displacement transducer was channeled through a bridge balance unit and then into the visicorder. The amplifier unit provided a means of amplifying more than one signal simultaneously and the visicorder oscillograph provided a means of representing these signals on photographic paper in a manner yielding the desired information. The paper used in the visicorder was standard Kodak linograph direct print paper in hundred foot lengths. The visicorder oscillograph ran at a speed of 80 inches per minute which was sufficient to capture the event and record it. A sample trace accompanied by a complete explanation is given in Appendix A.

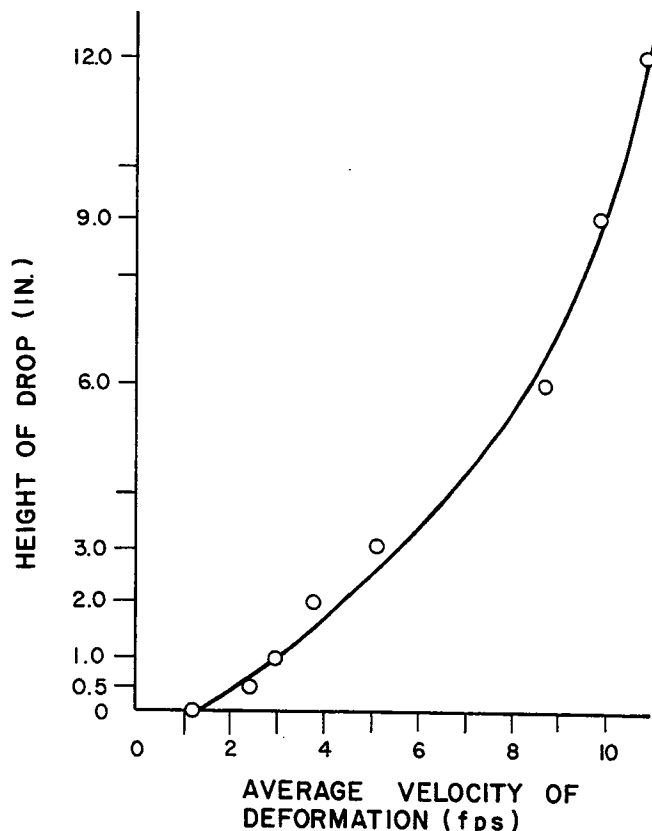


Figure 6. Average velocity of deformation versus height of drop.

Calibration of Equipment

In calibrating the load cells, the triaxial apparatus with no sample in it (top and bottom plates together) was placed in a static testing machine and incremental loads were placed on it ranging to more than those anticipated in the test. Each increment of load caused the deflection of a source of light on the photographic paper. Knowing the load and the resulting deflection, a calibration of load per unit of deflection could be calculated.

Calibration of the linear displacement transducer was accomplished by moving its shaft 0.1 inch or one revolution of an Ames dial then noting the deflection of the point light source on the photographic paper. An attenuation was obtained which gave the inches of movement of the point of light on the photographic paper per 0.1 inch of sample displacement. This attenuation was noted on each test record.

The pore pressure transducer was calibrated by attaching it to the triaxial base and applying varying cell pressures to get corresponding deflections of the light source on the photographic paper. By measuring the deflections of these light sources on the paper the calibration in inches of deflection per pound of pressure could be calculated.

Test Procedure

Procedures used in preparation of saturated sand samples were developed by Reeves (5), and used in this

study. The cohesive materials were tested in unconfined compression. They were remolded samples prepared by use of a Vac-aire extrusion machine, made by International Clay Machinery Company of Delaware, Model Laboratory, Serial No. A-843. Shiffert (9) did consid-

erable work with this machine and has shown that the samples produced are uniform. Raba (6) used some of Shiffert's samples and found them to be reliable. The samples used in this investigation were some of those prepared by Shiffert.

CHAPTER III

RESULTS OF TESTS ON SANDS

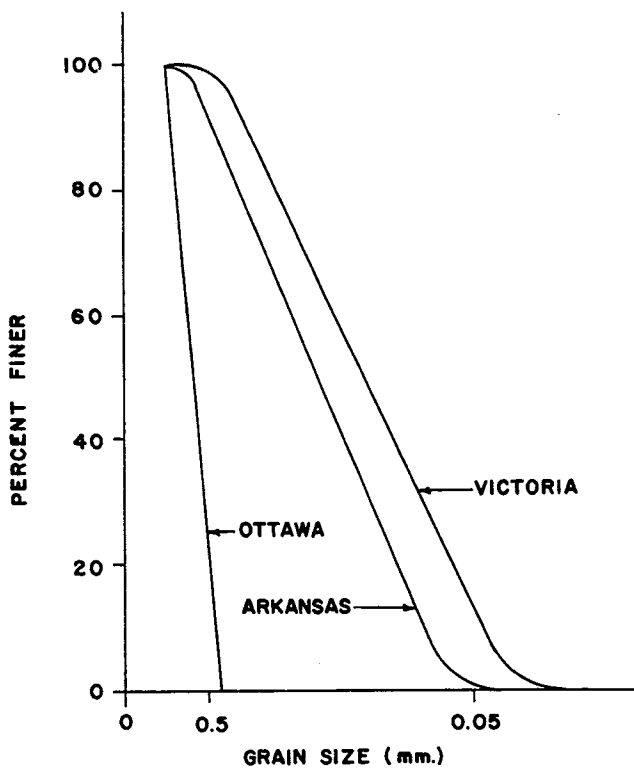
General

In testing the granular materials it was desired to get as wide a variation in physical properties as possible. A series of tests were conducted on Ottawa 20-30, Arkansas, and Victoria sands which vary in grain size and angularity of grains. Ottawa sand has uniform smooth grains; Arkansas sand has fine, angular grains; and Victoria sand has very fine and extremely angular grains. A grain size analysis is shown in Figure 7. Figure 8 shows a sample of Ottawa sand in the triaxial cell ready for impact.

It was desired to test these materials in the same manner so that comparisons of the damping constant could be made with certain properties of the sand. The dynamic tests performed were unconsolidated undrained tests, at a void ratio of 0.55, and a chamber pressure of 15 psi. Due to the method of sample preparation, the initial effective confining pressure was actually about -0.5 psi in the dynamic tests. The reason for this was that a 0.5 psi vacuum was applied during sample prepa-

ration (5). The static tests were performed consolidated drained, at a void ratio of 0.55 and a confining pressure of 15 psi. The dynamic tests were performed as undrained tests because at the instant of impact in driving a pile, it is felt that the water in the soil probably would not have time to drain. Conversely, the static tests were performed as drained tests because given sufficient time and a static loading the water in the soil would drain and the pore pressures would not develop.

A preliminary study was performed on Ottawa sand in which the void ratio was varied. The dynamic tests



were performed unconsolidated undrained, with a 15-psi chamber pressure and void ratios varying from 0.50 to 0.60. The static tests in this series were performed as consolidated drained tests with an effective confining pressure of 15 psi.

As mentioned in Chapter II, pore pressures were measured in the granular materials only in "pilot" tests to observe their behavior under dynamic loading. At the 0.55 void ratio pore pressure would plunge immediately upon impact to the limiting negative value (-14.7 psi) indicating cavitation of the sample. The pore pressure is, of course, integrally related to the degree of saturation of the sample. Considerable care was taken to prepare a sample which was 100% saturated. It is believed that this was accomplished since when the chamber pressure was increased by 15 psi, the pore pressure likewise increased by the same amount (-0.5 psi to 14.5 psi).

The samples were tested over a range of loading velocities varying from the minimum velocity obtainable to insure sample failure to a maximum velocity of 12 fps. Special care was taken at velocities of sample deformation of 0 - 3 fps to determine how the dynamic load varied with velocity in this range. Figure 9 shows values of peak dynamic load related to velocity of deformation for the three sands tested. The load increased very rapidly from zero velocity up to about 2 fps, then leveled off to a straight line with a slight slope which is essentially parallel for all three sands. A similar circumstance is seen when the ratio of dynamic to static load is related to velocity of deformation as shown in Figure 10.

Determination of a Constant Damping Value

With velocity of deformation and the ratio of dynamic to static load known, the damping constant, J , can be calculated from equation 4 by solving for this damping constant:

$$J = \frac{1}{V} \left[\frac{P_d}{P_s} - 1 \right] \quad (4a)$$

Using equation 4a with the experimental laboratory results of this investigation, calculated J values are shown in Figure 11. As seen in Figure 11, J is not a constant

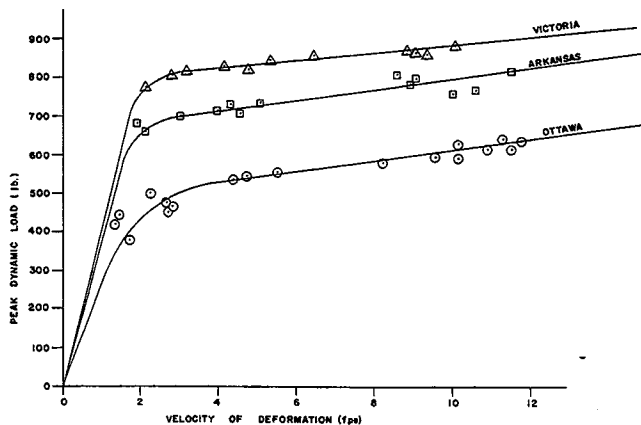


Figure 9. Velocity of sample deformation versus peak dynamic load for sands tested.

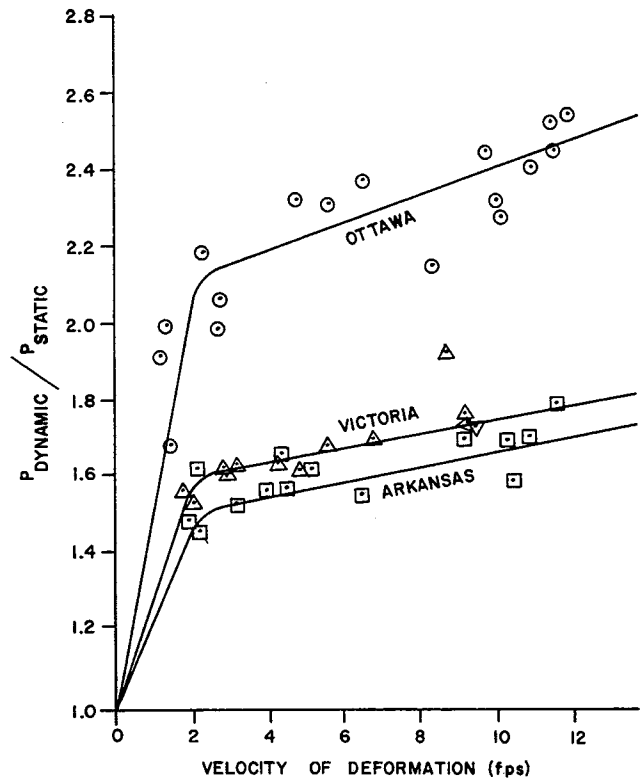


Figure 10. $P_{dynamic}/P_{static}$ versus velocity of deformation for sands tested.

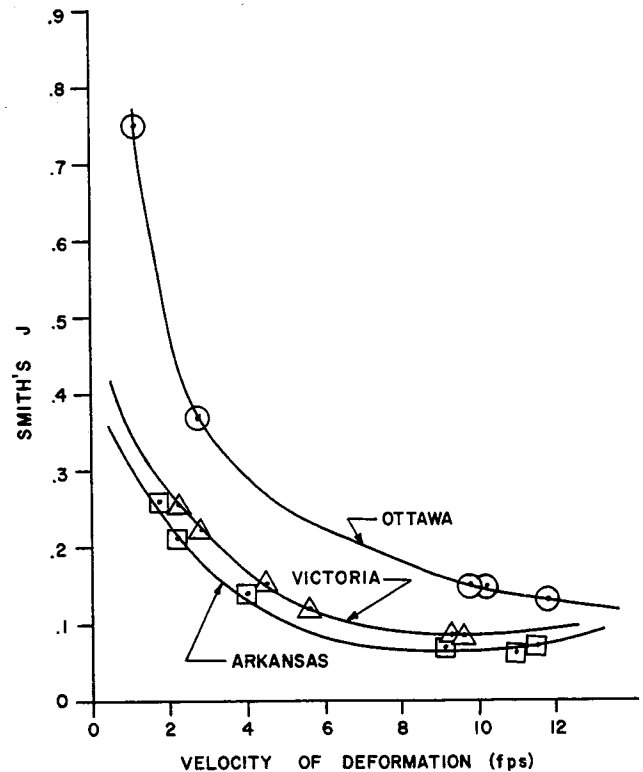


Figure 11. Smith's J versus velocity of deformation for sands tested.

but varies with velocity of deformation. In order to apply Smith's wave equation analysis (10) to the piling behavior problem J must be a constant. To obtain a constant J a modification of the original Smith equation was necessary. A reasonably constant value of J was found by raising velocity of deformation to some power less than one as follows:

$$J = \frac{1}{V^N} \left[\frac{P_d}{P_s} - 1 \right] \quad (6)$$

The results of raising velocity of deformation to a power using equation 6 may be seen in Tables I, II, and III, for the tests performed on granular materials. The values of constant J for the optimum N power are shown graphically in Figure 12 for all three sands. This J value remains constant over the full range of velocities.

It should be noticed from Tables I, II, and III, that Ottawa, Arkansas, and Victoria sands achieve a constant J value when velocity of deformation is raised to the $N = 0.21$, $N = 0.27$, and $N = 0.19$ powers, respectively. In Appendix B is shown a program for the digital computer which calculates values of J for the available data over a range of powers of velocity of deformation. Appendix B gives a detailed explanation of this program as well as instructions on its use.

It is desirable as a simplification to be able to represent all these materials to a common power of velocity of deformation. The power of $N = 0.20$ was chosen since less deviation from the optimum power resulted from choosing this power than any other. A thorough treatment of how the optimum power of velocity of deformation was chosen is taken up in Appendix C. Figure C-1 in this appendix illustrates graphically the effect of varying the power to which velocity of

Table I
RESULTS OF TESTS ON OTTAWA SAND

$e=0.55$ Condition—Saturated
 $\sigma_v=15$ psi
Type of Test—unconsolidated N(optimum)—0.21
undrained
 $P_s=228.1$ pounds Average J—0.92

Height of Drop	Velocity of Deformation	Dynamic Load	$\frac{P_d}{P_s}$	J for V^{optimum}	J for $V^{.20}$
Inches	ft/sec	pounds			
0.0625	1.25	443.0	1.94	0.90	0.90
0.125	1.43	461.0	2.02	0.95	0.95
0.25	1.55	390.0	1.71	0.65	0.65
0.5	2.75	477.0	2.09	0.88	0.89
1.0	2.37	504.0	2.21	1.01	1.02
1.0	2.84	477.0	2.09	0.88	0.87
1.0	2.70	461.0	2.02	0.83	0.84
3.0	5.65	533.0	2.33	0.93	0.94
3.0	4.56	532.0	2.33	0.97	0.99
3.0	4.85	537.0	2.35	0.97	0.93
9.0	8.39	553.5	2.39	0.91	0.93
9.0	10.02	537.0	2.35	0.84	0.85
9.0	9.75	566.0	2.48	0.92	0.94
12.0	10.95	561.5	2.46	0.88	0.90
12.0	10.16	586.0	2.57	0.96	0.99
12.0	11.40	585.0	2.57	0.94	0.96
12.0	11.56	566.5	2.48	0.89	0.91
12.0	11.85	580.5	2.54	0.92	0.94

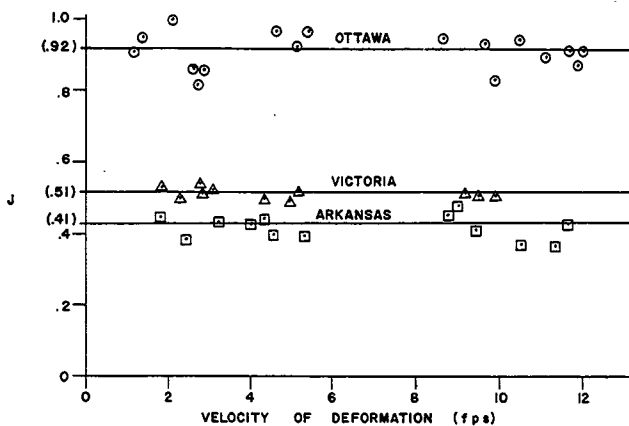


Figure 12. Damping constant versus velocity of deformation raised to the optimum power for sands tested.

Table II

RESULTS OF TESTS ON ARKANSAS SAND

$e=0.55$ Condition—saturated
 $\sigma_v=15$ psi
Type of Test—Unconsolidated N(optimum) = 0.27
undrained
 P_s (drained)—459.7 Average J = 0.41

Height of Drop	Velocity of Deformation	Dynamic Load P_d	$\frac{P_d}{P_s}$	J for V^{optimum}	J for $V^{.20}$
Inches	ft/sec	pounds			
0.5	1.94	696.0	1.515	0.43	0.45
1.0	3.12	714.0	1.554	0.41	0.44
2.0	2.20	673.0	1.466	0.38	0.40
3.0	4.00	730.5	1.591	0.41	0.45
3.0	4.57	734.0	1.599	0.40	0.44
3.0	4.41	754.5	1.641	0.43	0.48
3.0	5.24	757.0	1.650	0.41	0.46
6.0	9.17	802.5	1.750	0.41	0.48
9.0	9.27	812.5	1.770	0.42	0.49
9.0	8.65	822.0	1.792	0.44	0.51
12.0	10.90	798.5	1.740	0.39	0.46
12.0	10.30	797.0	1.739	0.39	0.46
12.0	11.60	835.0	1.821	0.42	0.50

Table III

RESULTS OF TESTS ON VICTORIA SAND

$e=0.55$ Condition—saturated
 $\sigma_v=15$ psi
Type of Test—unconsolidated N(optimum)—0.19
undrained
 P_s (drained)—498 pounds Average J—0.51

Height of Drop	Velocity of Deformation	Dynamic Load P_d	$\frac{P_d}{P_s}$	J for V^{optimum}	J for $V^{.20}$
Inches	ft/sec	pounds			
0.5	2.12	773.0	1.51	0.48	0.48
1.0	1.80	786.0	1.58	0.52	0.51
1.0	3.20	824.0	1.65	0.52	0.52
2.0	2.87	819.0	1.65	0.53	0.52
2.0	2.93	809.0	1.67	0.51	0.50
3.0	4.32	823.0	1.65	0.50	0.49
3.0	4.95	818.0	1.64	0.48	0.47
6.0	5.58	849.0	1.71	0.51	0.50
9.0	9.20	889.0	1.78	0.51	0.50
9.0	9.50	879.0	1.76	0.50	0.49
12.0	9.28	884.0	1.77	0.51	0.50

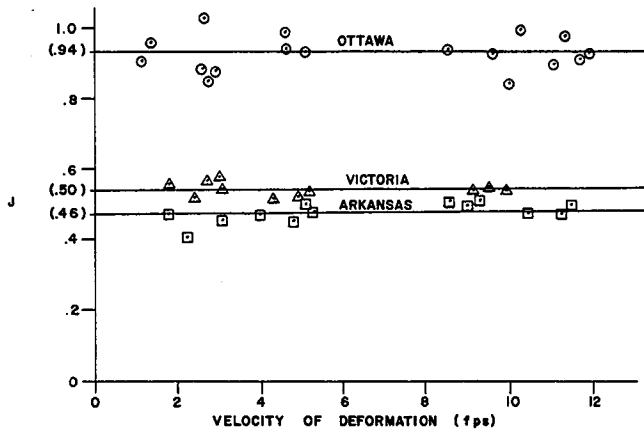


Figure 13. Damping constant versus velocity of deformation raised to the .20 power for sands tested.

deformation may be raised. Figure 13 shows J related to velocity of deformation for all three sands for the power $N = 0.20$. Tables I, II, and III show a tabulation of these values.

Comparing J values in these tables where velocity of deformation is raised to the optimum and $N = 0.20$, it is seen that only slight changes occur in the J values. Table IV shows quantitatively in Part A the error involved when velocity of deformation is raised to the optimum power and in Part B the error involved when velocity of deformation is raised to the $N = 0.20$ power. It is seen that the error shown in this table is, in both cases, well within the bounds of experimental accuracy. The additional error which results when velocity of deformation is changed from the optimum to the $N = 0.20$ power is not prohibitive.

Damping Constant Related to Certain Sand Properties

It is desirable to have damping constant values related to some property of the sand itself. Effective

Table IV
ERROR RESULTING FROM APPROXIMATIONS
A. Results of J Values for $N = \text{optimum}$

	Ottawa	Arkansas	Victoria
Average J	0.92	0.41	0.51
Power of velocity	0.21	0.27	0.19
Max + deviation (%) from average J	9.90	7.30	3.90
Max - deviation (%) from average J	29.50	7.30	5.90
Average deviation (%) from average J	4.27	5.15	3.36

B. Results of J Values for $N = 0.20$

	Ottawa	Arkansas	Victoria
Average J	0.94	0.46	0.50
Max + deviation (%) from average J	8.50	10.80	4.00
Max - deviation (%) from average J	30.40	10.80	6.00
Average deviation (%) from average J	4.65	6.09	3.40

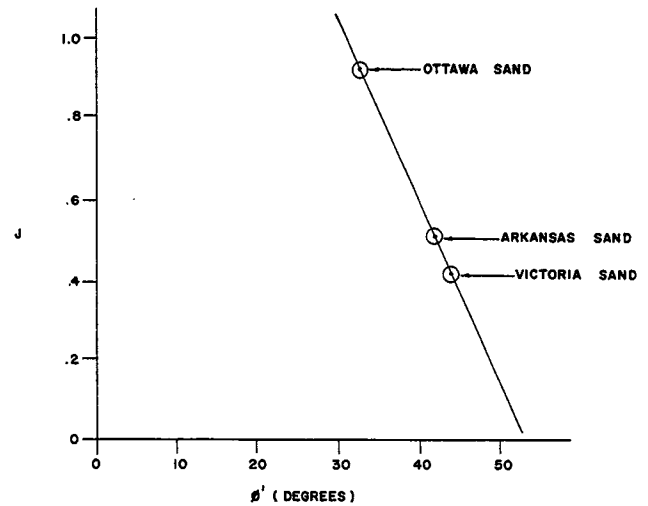


Figure 14. Effective angle of internal shearing resistance versus damping constant for sands tested.

angle of internal shearing resistance from static tests was related to the damping constant, J . There was some question concerning the validity of relating ϕ' from static tests to J obtained from dynamic tests. Nishida (4) shows the angle of internal shearing resistance to be different at both the top and bottom of the sample. Whitman and Healy (12) have shown the difference in dynamic and static angle of internal shearing resistance to be less than one degree. This slight difference is not considered significant in this investigation. Appendix D shows detailed Mohr Circle diagrams obtained from static tests for each sand. The ϕ' value was obtained from drained tests and from undrained tests with pore pressure measurements. Figure 14 shows J related to ϕ' for Ottawa, Arkansas and Victoria sands.

For the study in which void ratio was varied to determine its effect on J , only a limited number of tests were performed. Tests were performed at two heights of drop with a primary objective of defining the relation between peak load and velocity of sample deformation as shown in Figure 15. The sample at $e = 0.6$ was difficult to prepare because of its extremely loose packing of grains and it consolidated somewhat even under the

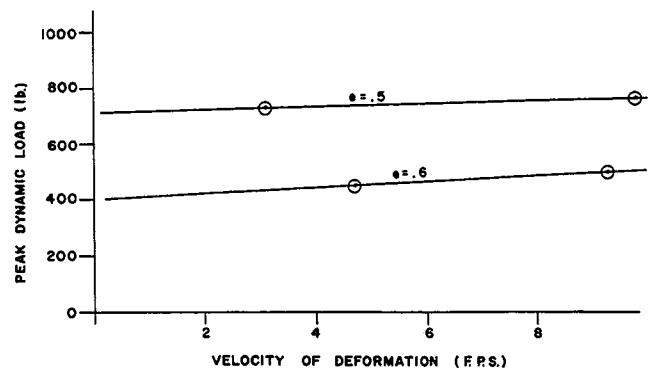


Figure 15. Peak dynamic load versus velocity of deformation for void ratio study on Ottawa Sand.

0.5 psi vacuum necessary to prepare the sample. Table V shows the average dynamic load and velocity of deformation values obtained for $e = 0.5$ tests and $e = 0.6$ tests. Complete information on the $e = 0.55$ tests appears in Table I.

The optimum powers of velocity of deformation to obtain a constant J for the $e = 0.5$ and $e = 0.6$ tests lie quite far from the assumed average value of $N = 0.20$ as seen in Table V. Tables I and III give all pertinent information on the $e = 0.55$ tests. Figure 16 shows a considerable deviation in J values which results when velocity of deformation is represented to both the optimum and average values. The major deviations in J values from the average are seen to occur at the loosest void ratio of $e = 0.6$. It is felt that if a pile were driven in sands with a void ratio as loose as $e = 0.6$, the sands would consolidate to a denser void ratio during driving. Thus, considering the denser void ratios in Figure 16, the average J values shown by representing velocity of deformation to the $N = 0.20$ power are reasonable.

Table V
STUDY OF VOID RATIO CHANGE IN OTTAWA SAND

A. $e = 0.5$					
Type of Test—consolidated undrained			Condition—saturated		
$\sigma_s = 15$ psi			$N(\text{optimum}) = 0.10$		
P_s (drained) = 322 pounds					
Height of Drop	Average Velocity of Deformation	Average Dynamic Load	$\frac{P_d}{P_s}$	J for $N = \text{optimum}$	J for $N = 0.20$
Inches	ft/sec	pounds			
3.0	3.19	715.0	2.23	1.09	0.97
9.0	9.80	762.0	2.38	1.09	0.87

B. $e = 0.6$					
P_s (drained) = 218 pounds			$N(\text{optimum}) = .43$		
Height of Drop	Average Velocity of Deformation	Average Dynamic Load	$\frac{P_d}{P_s}$	J for $N = \text{optimum}$	J for $N = .20$
Inches	ft/sec	pounds			
3.0	4.70	460.0	2.11	0.57	0.82
9.0	9.30	542.5	2.48	0.57	0.95

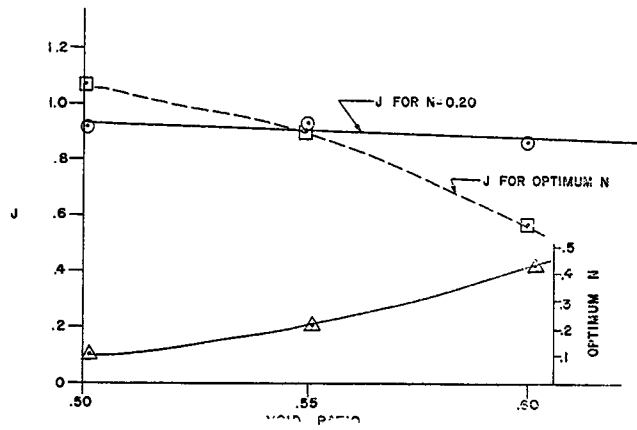


Figure 16. Void ratio versus damping constant for Ottawa sand.

The significance of these relationships is that in clean sands if the void ratio of a particular material or the effective angle of internal shearing resistance is known, a good approximation of a J value may be made.

Summary of Results

This chapter has dealt with tests performed on three granular materials. The objectives of these tests were to determine soil damping constants by performing impact tests and to correlate these soil damping constants with common soil properties such as angle of internal shearing resistance and void ratio.

To produce this correlation, a series of impact tests were performed and sufficient data gathered such that J values could be calculated. A modification in Smith's equation was made by raising velocity of deformation to an optimum power in order to obtain a J value which was constant. Once an optimum power of velocity of sample deformation was obtained, an average power was determined which was convenient for all sands tested. This average power of velocity of deformation was the 0.20 power. The resulting average J value was related to effective angle of internal shearing resistance for the three granular materials tested.

To relate void ratio and damping constant, J , tests were performed at three different void ratios on Ottawa sand. The same modification in the Smith equation was made and determination of an average power ($N = 0.20$) of velocity of deformation was similarly accomplished. Void ratio was then related to the average value of damping constant, J , for the three void ratios investigated.

CHAPTER IV

RESULTS OF TESTS ON CLAYS

General

In the cohesive materials, it was again important to select soils with variable properties. Figure 17 shows the location of the materials on the plasticity chart. It can be seen that they are spread across the chart with all

but Hall Pit clay being CH materials. The samples were cured in the moisture room for sufficient time to obtain maximum strength. The materials tested were: organic clay, Vettors clay, Easterwood clay, and Hall Pit sandy clay. The failure modes of the Vettors material may be seen in Figure 18. Note how the dryer materials such

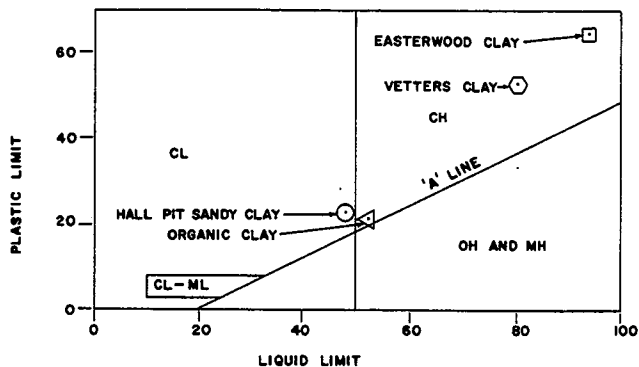


Figure 17. Location on plasticity chart of clays tested.

as VE 46 fail by cracking whereas the wetter materials such as VE 55 fail by bulging. These modes of failure become even more pronounced as the material's moisture content becomes either wetter or dryer than those shown for Veters clay.

These materials were tested in the same manner so that comparisons of their properties could be made. The dynamic tests were unconsolidated undrained tests with no confining pressure. The static tests were a standard unconfined compression test. There was some question concerning the effect of confining pressure during impact tests on these soils, therefore a preliminary study of this effect was initiated on organic clay at a moisture content of 37 percent. As shown in Figure 19, the effect of confining pressure was minimal and was not considered further in this study.

A tabulation of the data for this study is seen in Table VIII. The sample size used in the dynamic tests was 2.8 inches in diameter and 3 1/4 inches long. It was desirable to use a short sample since the number of available samples was limited. Again a preliminary investigation was undertaken to study the effects of sample height on impact test results. The material tested was organic clay at a moisture content of 36%. This study indicated that a 3 1/4-inch sample could be used and would yield significantly the same result as the 6-inch sample. This information is presented graphically in Figure 20. The static tests were run with samples 2.8 inches in diameter and 6 inches long in accordance with standard unconfined compression test procedures.

The cohesive materials were tested over a range of loading velocities of 0-12 fps. Data were reduced from

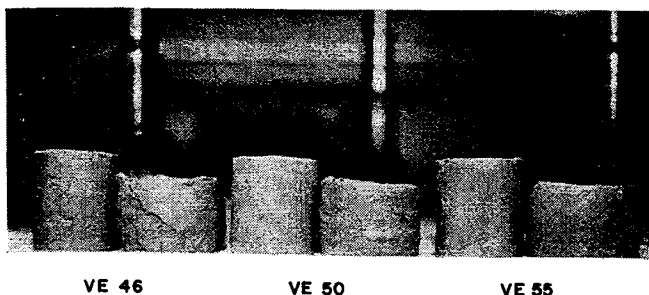


Figure 18. Vetter's clay at three moisture contents before and after failure.

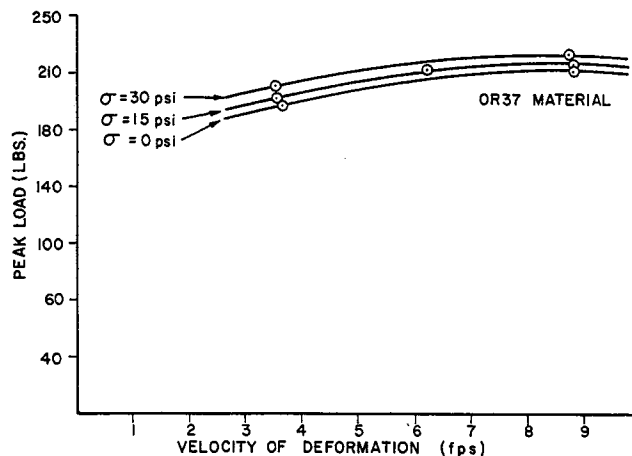


Figure 19. Effect of confining pressure on OR 37 material.

the visicorder trace in the same manner as were the sands. Again, reference is made to Appendix A for a complete explanation of the data reduction process and a sample visicorder trace. Figure 21 shows values of peak dynamic load related to velocity of deformation for the cohesive materials. The dynamic load in the cohesive materials increases sharply to a limiting value then takes the form of a smooth curve. Figure 22 shows values of the ratio of dynamic to static load related to velocity of deformation.

Determination of a Constant Damping Value

Using equation 4a:

$$J = \frac{1}{V} \left[\frac{P_d}{P_s} - 1 \right]$$

and using the test results of this investigation, Smith's computed J values can be found. A typical curve of Smith's J related to velocity of deformation is shown in Figure 23 for EA 50 material. As in the sands, Smith's damping value is a variable. It must be made a constant value if it is to serve as a damping constant.

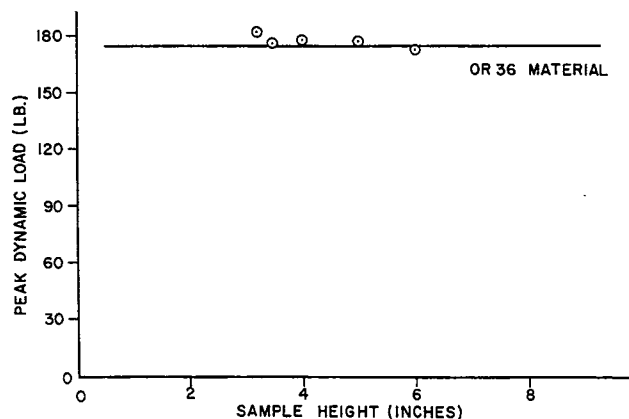


Figure 20. Effect of sample height on dynamic load in OR 36 material.

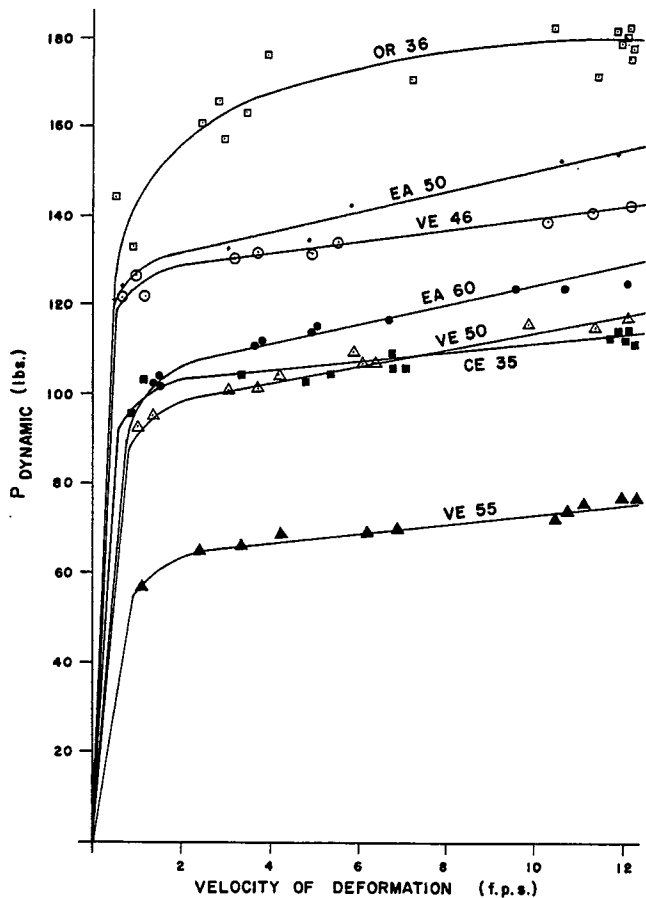


Figure 21. Dynamic load versus velocity of deformation for clays tested.

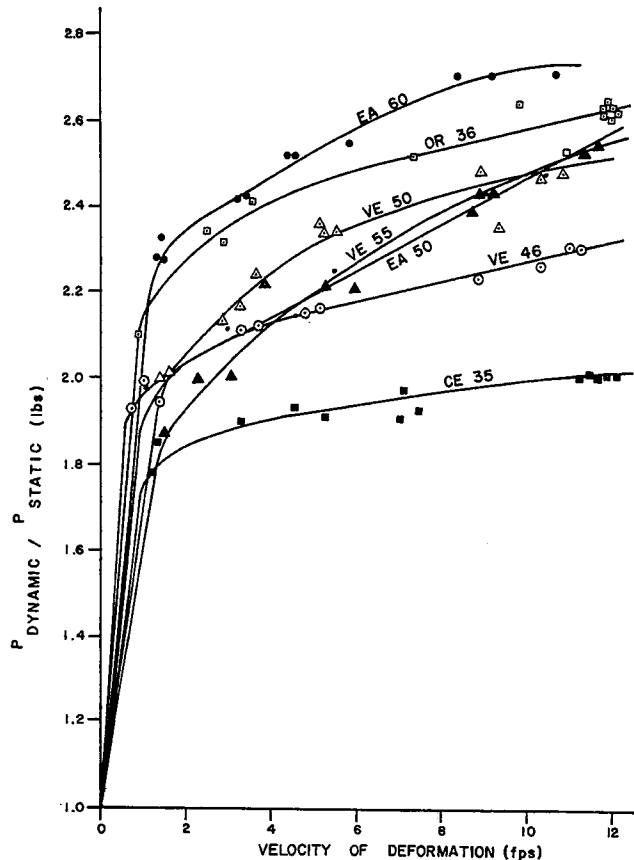


Figure 22. Ratio of dynamic to static load versus velocity of deformation for clays tested.

By modifying Smith's equation, raising velocity of deformation to some power, a reasonably constant value of J for the clay materials can be obtained. Equation 6 is applicable for this purpose:

$$J = \frac{1}{\sqrt{N}} \left[\frac{P_d}{P_s} - 1 \right] \quad (6)$$

Tables VI through XVI show all relevant data pertaining to the tests on cohesive materials. It can be seen that

Table VI
RESULTS OF TESTS ON OR 31 CLAY*

Type of Test—unconsolidated undrained N(optimum) = 0.18
 Confining Pressure—none
 P_{static}—105 pounds Average J = 0.749
 Moisture Content = 31%

Velocity of Drop	Height of Deformation	Dynamic Load	$\frac{P_d}{P_s}$	J for N = optimum	J for N = 0.18
Inches	ft/sec	pounds			
3.0	4.05	206.0	1.96	0.748	0.748
6.0	7.00	217.0	2.06	0.751	0.751
9.0	8.75	221.0	2.10	0.748	0.748

*Test performed in Fall of 1967.

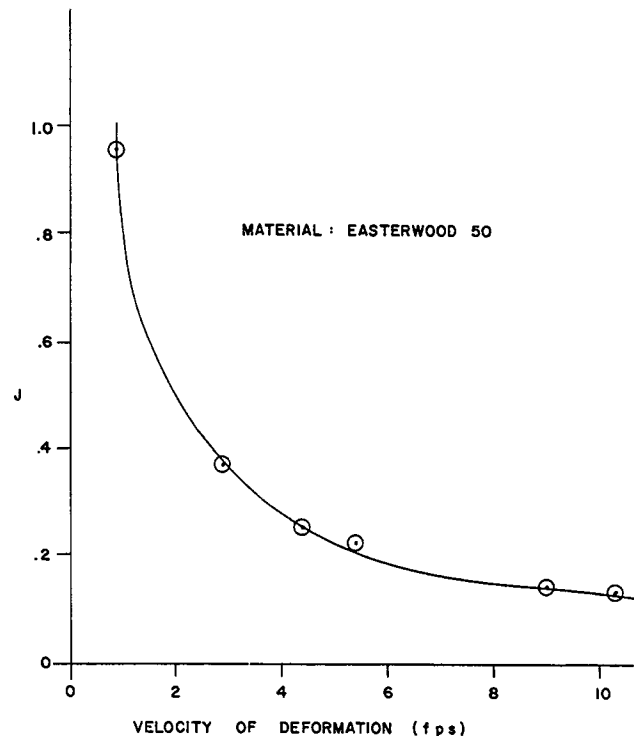


Figure 23. Smith's J versus velocity of deformation for EA 50 material.

there is variation in the data especially pertaining to values of J and the optimum power to which velocity of deformation must be raised. Again, as a simplification, velocity of deformation must be represented to one common power for all clays. The overall optimum power of velocity of deformation is $N = 0.18$ for the cohesive materials tested. This power is not an average value but rather a number arrived at by inspecting the relative change in the data brought about by a change in power of velocity of deformation. Some data are closer to the optimum value and changing the exponent causes little alteration whereas the opposite effect is observed from data whose optimum power is farther from $N = 0.18$. Tables VI through XVI show a tabulation of J values represented to both the optimum N and $N = 0.18$ powers. From these tables it can be seen that little change in the values of J was wrought

Table VII
RESULTS OF TESTS ON OR 36 CLAY

Type of test—unconsolidated undrained $N(\text{optimum}) = 0.22$
 Confining Pressure—none
 $P_{\text{static}} = 67.75$ pounds Average J = 0.995
 Moisture Content = 33.6%

Height of Drop	Velocity of Deformation	Dynamic Load	$\frac{P_d}{P_s}$	J for N = optimum	J for N = 0.18
Inches	ft/sec	pounds			
0.0	1.28	132.0	2.11	1.05	1.05
0.5	2.43	161.0	2.38	1.14	1.18
1.0	2.77	158.0	2.34	1.06	1.11
2.0	3.28	163.0	2.41	1.08	1.14
3.0	6.33	170.0	2.51	1.01	1.08
6.0	8.68	180.0	2.66	1.04	1.13
9.0	10.33	181.0	2.67	1.00	1.10
9.0	10.58	178.0	2.63	0.97	1.07
9.0	9.60	172.0	2.54	0.94	1.02
9.0	10.25	178.5	2.63	0.98	1.08
9.0	10.42	177.0	2.62	0.96	1.06
12.0	10.22	179.5	2.65	0.99	1.05
12.0	10.32	179.5	2.65	0.99	1.08

Table VIII
RESULTS OF TESTS ON OR 37 CLAY AND STUDY OF EFFECT OF CONFINING PRESSURE*

Type of Test—unconsolidated undrained $N(\text{optimum}) = 0.20$
 P_{static} at $\sigma_3 = 0$ 59 pounds Average J = 0.837
 P_{static} at $\sigma_3 = 15$ 67 pounds
 P_{static} at $\sigma_3 = 30$ 71 pounds
 Moisture Content = 37%

Confining Pressure	Height of Drop	Velocity of Deformation	Dynamic Load	$\frac{P_d}{P_s}$	J for N = optimum	J for N = 0.18
psi	Inches	ft/sec	pounds			
0	3.0	4.00	124.0	2.10	0.835	0.858
0	6.0	6.03	130.0	2.20	0.840	0.871
0	9.0	9.20	136.0	2.30	0.837	0.875
15	3.0	3.90	130.0			
15	6.0	6.45	136.0			
15	9.0	8.10	138.0			
30	3.0	3.61	130.0			
30	9.0	8.42	140.0			

*Tests performed in Fall 1967.

Table IX
RESULTS OF TESTS ON EA 62 CLAY*

Type of Test—unconsolidated undrained $N(\text{optimum}) = 0.16$
 Confining Pressure—none Average J = 1.16
 $P_{\text{static}} = 42$ pounds
 Moisture Content = 62%

Height of Drop	Velocity of Deformation	Dynamic Load	$\frac{P_d}{P_s}$	J for N = optimum	J for N = 0.18
Inches	ft/sec	pounds			
3.0	3.75	102.0	2.43	1.16	1.13
6.0	6.15	108.0	2.58	1.18	1.13
9.0	9.00	111.0	2.64	1.16	1.11

*Tests performed in Fall of 1967.

Table X
RESULTS OF TESTS ON EA 60 CLAY

Type of Test—unconsolidated undrained $N(\text{optimum}) = 0.15$
 Confining Pressure—none Average J = 1.23
 $P_{\text{static}} = 45.25$ pounds
 Moisture Content = 59.43%

Height of Drop	Velocity of Deformation	Dynamic Load	$\frac{P_d}{P_s}$	J for N = optimum	J for N = 0.18
Inches	ft/sec	pounds			
0.0	1.44	103.2	2.28	1.21	1.20
0.0	1.41	103.3	2.28	1.22	1.21
0.0	1.43	106.2	2.35	1.28	1.26
1.0	3.32	111.4	2.46	1.22	1.18
1.0	3.26	111.0	2.45	1.22	1.18
2.0	4.30	114.0	2.52	1.22	1.17
3.0	4.36	114.2	2.52	1.22	1.17
3.0	5.93	116.0	2.56	1.20	1.14
6.0	8.30	124.0	2.74	1.27	1.19
9.0	9.32	124.0	2.74	1.25	1.16
9.0	10.65	124.0	2.74	1.22	1.14

Table XI
RESULTS OF TESTS ON EA 55 CLAY*

Type of Test—unconsolidated undrained
 Confining Pressure none
 $P_{static} = 71$ pounds
 Moisture Content = 55%
 $N(\text{optimum}) = 0.20$
 Average $J = .497$

Height of Drop Inches	Velocity of Deformation ft/sec	Dynamic Load pounds	$\frac{P_d}{P_s}$	J for N = optimum	J for N = 0.18
				0.945	0.974
3.0	3.58	158.0	2.23	0.945	0.974
6.0	6.65	170.0	2.40	0.955	0.991
9.0	8.95	175.0	2.47	0.945	0.987

*Tests performed in Fall 1967.

by modifying N to the common $N = 0.18$ power. This may be seen graphically in Figures 24 and 25. Figure 24 shows J related to velocity of deformation raised to the optimum power for the materials tested. Figure 25 shows for all materials tested, the J value related to velocity of deformation raised to the 0.18 power. This same change in J values may be seen quantitatively in Table XVII. In this table the change in damping constant is shown as an increase in percent deviation from

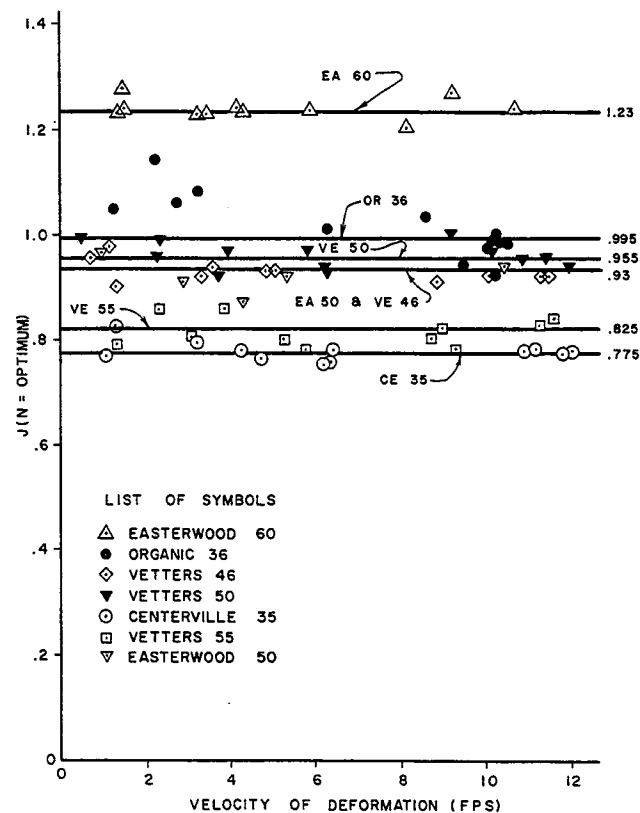


Figure 24. Damping constant at $N = \text{optimum}$ versus velocity of deformation for clays.

Table XII
RESULTS OF TESTS ON EA 50 CLAY

Type of Test—unconsolidated undrained
 Confining Pressure none
 $P_{static} = 63.5$ pounds
 Moisture Content = 48.9%
 $N(\text{optimum}) = 0.19$
 Average $J = 0.93$

Height of Drop Inches	Velocity of Deformation ft/sec	Dynamic Load pounds	$\frac{P_d}{P_s}$	J for N = optimum	J for N = 0.18
				0.97	0.97
0.0	1.00	125.0	1.97	0.97	0.97
1.0	2.90	134.5	2.12	0.91	0.92
2.0	4.40	136.4	2.15	0.87	0.88
3.0	5.48	144.0	2.27	0.92	0.93
9.0	9.04	154.0	2.43	0.94	0.96
12.0	10.32	156.0	2.46	0.94	0.96

the average J value for velocity of deformation raised to both optimum and 0.18 powers.

Damping Constant Related to Certain Clay Properties

With all tests having been performed in the same manner and all soils having been represented in the same manner, comparisons may be made. Figure 26

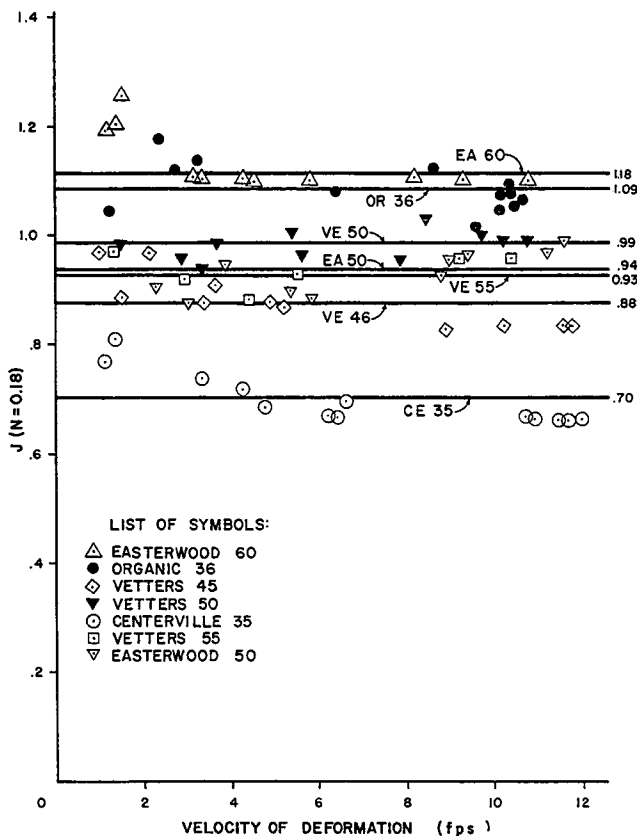


Figure 25. Damping constant at $N = 0.18$ versus velocity of deformation for clays tested.

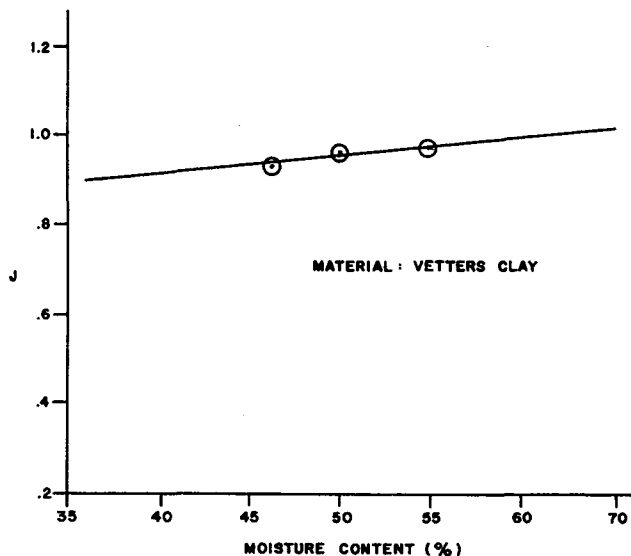


Figure 26. Moisture content versus damping constant for Vettters clay.

shows moisture content related to J for Vettters clay. The relationship is a straight line. Similar data could be shown for all clays tested. Figure 27 shows damping constant, J, related to liquidity index. Liquidity index is defined as:

$$L.I. = \frac{\text{Moisture Constant} - \text{Plastic Limit}}{\text{Plasticity Index}}$$

Liquidity index is sometimes referred to in literature as the water-plasticity ratio.

Table XIII
RESULTS OF TESTS ON VE 55 CLAY

Type of Test—unconsolidated undrained
 Confining Pressure—none
 P_{static} Fall 1967—30.7 pounds
 Spring 1968—31.16 pounds
 Moisture Content = 55.32%

$N(\text{optimum}) = 0.25$
 Average J = 0.825

Height of Drop	Velocity of Deformation	Dynamic Load	$\frac{P_d}{P_s}$	J for N = optimum	J for N = 0.18
Inches	ft/sec	pounds			
*0.0	0.175	59.0	1.92	0.80	0.87
0.0	1.380	57.8	1.86	0.79	0.81
0.5	2.230	64.0	2.055	0.86	0.91
1.0	3.060	64.2	2.06	0.80	0.88
1.5	3.900	69.0	2.22	0.86	0.95
*1.5	3.530	69.0	2.245	0.91	0.99
3.0	5.310	69.0	2.22	0.80	0.90
3.0	5.810	69.0	2.22	0.78	0.89
*3.0	6.000	73.0	2.38	0.88	1.00
6.0	9.340	76.2	2.45	0.83	0.97
*9.0	7.950	75.0	2.44	0.99	0.86
9.0	8.750	74.0	2.37	0.80	0.93
12.0	11.450	78.5	2.52	0.83	0.98
12.0	9.000	75.5	2.42	0.82	0.96
12.0	11.650	79.5	2.55	0.84	1.00

*Tests performed in Fall 1967.

Table XIV
RESULTS OF TESTS ON VE 50 CLAY

Type of Test—unconsolidated undrained
 Confining Pressure—none
 P_{static} Fall 1967—42.5 pounds
 Spring 1968—47.0 pounds
 Moisture Content = 49.01%

$N(\text{optimum}) = 0.20$
 Average J = 0.955

Height of Drop	Velocity of Deformation	Dynamic Load	$\frac{P_d}{P_s}$	J for N = optimum	J for N = 0.18
Inches	ft/sec	pounds			
*0.0	0.70	80.0	1.88	0.95	0.95
0.0	1.30	94.6	2.01	0.96	0.97
0.0	1.36	96.3	2.05	0.99	0.99
1.0	3.36	102.0	2.17	0.92	0.94
1.0	2.80	101.0	2.15	0.94	0.96
2.0	3.70	106.0	2.25	0.97	0.99
*3.0	4.37	94.0	2.21	0.90	0.93
3.0	5.60	109.1	2.32	0.94	0.97
3.0	5.31	110.9	2.36	0.97	1.01
3.0	5.78	109.0	2.32	0.93	0.96
*6.0	6.72	99.0	2.33	0.91	0.94
6.0	9.60	119.0	2.36	0.97	1.02
6.0	8.66	119.0	2.53	1.00	1.04
*6.0	8.50	101.0	2.40	0.90	0.94
9.0	10.82	119.0	2.53	0.95	1.00
9.0	10.23	118.2	2.52	0.95	1.00

*Tests performed in Fall of 1967.

This value is considered an important property of the material because it includes Atterburg's limits as well as the moisture content of the material. The information in Figure 27 appears duplicated since one material may be represented by two points. The reason for this is that

Table XV
RESULTS OF TESTS ON VE 46 CLAY

Type of test—unconsolidated undrained
 Confining Pressure—none
 P_{static} Fall 1967 = 56.5 pounds
 Spring 1968 = 63.0 pounds
 Moisture Content—45.54%

$N(\text{optimum}) = 0.14$
 Average J = 0.93

Height of Drop	Velocity of Deformation	Dynamic Load	$\frac{P_d}{P_s}$	J for N = optimum	J for N = 0.18
Inches	ft/sec	pounds			
*0.0	0.78	102.0	1.80	0.84	0.84
0.0	0.83	122.0	1.94	0.96	0.97
0.0	1.40	122.5	1.95	0.90	0.89
0.0	1.20	126.0	2.00	0.98	0.97
0.5	3.39	132.0	2.10	0.92	0.88
1.0	3.60	133.8	2.12	0.94	0.89
*3.0	4.18	121.0	2.14	0.93	0.89
3.0	5.16	137.0	2.18	0.93	0.87
3.0	4.90	136.5	2.17	0.93	0.88
*6.0	6.74	128.0	2.26	0.97	0.90
6.0	8.90	140.5	2.23	0.91	0.83
*9.0	7.87	130.0	2.30	0.98	0.90
9.0	10.24	143.0	2.27	0.92	0.84
12.0	11.38	144.5	2.30	0.92	0.84
12.0	11.38	144.5	2.30	0.92	0.84

*Tests performed in Fall 1967.

Table XVI

RESULTS OF TESTS ON HALL PIT SANDY-CLAY

Type of Test—unconsolidated undrained
 Confining Pressure—none
 $P_{static} = 55.3$ pounds
 Moisture Content = 34.68%

$N(\text{optimum}) = 0.11$
 Average $J = 0.775$

Height of Drop Inches	Velocity of Deformation ft/sec	Dynamic Load pounds	$\frac{P_d}{P_s}$	J for N = optimum	J for N = 0.18
0.0	1.45	103.0	1.86	0.83	0.81
0.0	1.10	98.4	1.78	0.77	0.77
1.0	3.29	105.8	1.91	0.79	0.74
2.0	4.84	105.8	1.91	0.76	0.69
2.0	4.25	106.9	1.93	0.78	0.72
3.0	6.27	107.0	1.93	0.75	0.67
3.0	6.20	107.0	1.93	0.75	0.67
3.0	6.375	109.1	1.98	0.78	0.70
9.0	10.73	112.2	2.03	0.77	0.67
9.0	11.65	112.8	2.04	0.77	0.67
12.0	11.68	113.0	2.04	0.78	0.67
12.0	11.65	112.8	2.04	0.77	0.67
12.0	11.30	113.0	2.04	0.78	0.67

the tests were performed at two different times: the earlier time being the Fall of 1967 and the latter the Spring of 1968. Generally the tests performed in 1968 lie above the earlier ones because of thixotropic hardening which occurred in the material. OR 36 was prepared at a different time and moisture content than the other organic materials shown in Figure 27 and thus no relationship exists between these soils.

The data in Figure 27 are represented as a band since several materials are involved. The dotted lines show the maximum deviation in J values which could be expected across the band at a given liquidity index. The maximum error in selected J values which could result is about 12 percent.

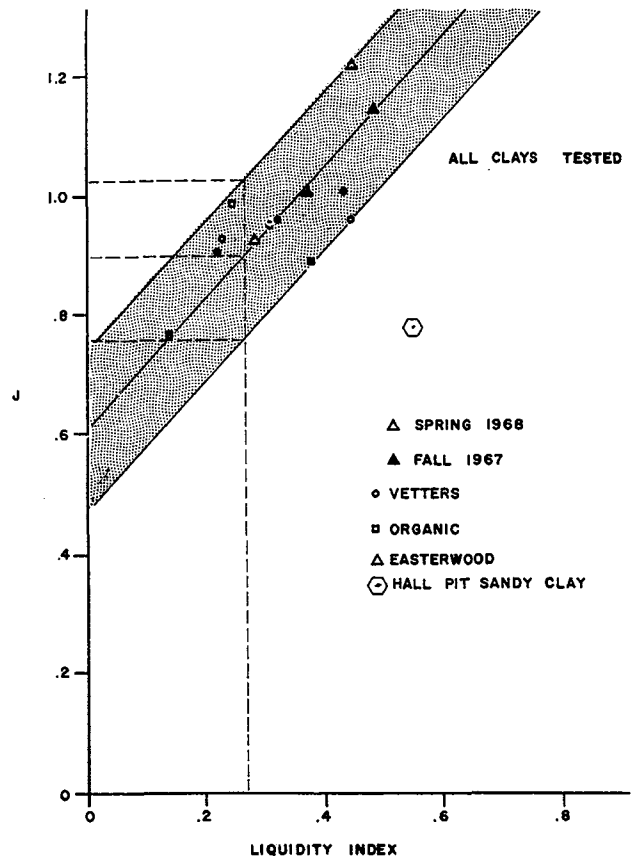


Figure 27. Liquidity index versus damping constant for clays tested.

Hall Pit sandy clay does not fit in this band of materials. As seen in Figure 17 this material is the only one of the soils tested which is not a CH material. Thus the band which was defined in Figure 27 appears to be valid only for CH materials. It was desirable to test this

Table XVII
 ERROR RESULTING FROM APPROXIMATIONS RESULTS OF J VALUES FOR N = 0.18

	OR 36	EA60	EA50	VE55	VE50	VE46	CE35
Average J	1.09	1.18	0.94	0.93	0.99	0.88	0.700
Max + deviation (%) from average J	8.28	6.78	3.20	12.90	5.05	10.20	5.700
Max - deviation (%) from average J	6.42	3.39	6.40	7.53	5.05	5.70	4.280
Avg. deviation (%) from average J	3.11	2.00	2.84	4.60	2.27	3.92	5.050

RESULTS OF J VALUES FOR N = OPTIMUM

	OR 36	EA60	EA50	VE55	VE50	VE46	CE35
Average J	0.995	1.23	0.93	0.825	0.955	0.93	0.775
Power of velocity of Deformation	0.220	0.15	0.19	0.250	0.200	0.14	0.110
Max + deviation (%) from average J	14.700	4.06	4.30	4.230	4.710	5.38	7.100
Max - deviation (%) from average J	5.560	2.44	6.45	5.450	3.660	3.22	3.230
Avg. deviation (%) from average J	3.080	1.62	1.76	2.320	1.750	1.64	1.740

material in order to define the boundaries of the relationships obtained. The band of Figure 27 likely defines the band of CH materials since the soils which lie in it are well spread across the CH portion of the plasticity chart.

The significance of these relationships are that if certain properties of the material are known such as moisture content and Atterburg limits, a good approximation of J value can be made.

Summary of Results

This chapter dealt with tests performed on organic clay, Easterwood clay, Veters clay and Hall Pit sandy clay. The objectives of these tests were to determine

soil damping constants related to soil properties such as moisture content and liquidity index.

To correlate moisture content and liquidity index with the damping constant, J, a series of impact tests were performed and sufficient data gathered to calculate J values. As in the sand tests, Smith's J value varied with velocity of deformation. It was necessary to modify Smith's equation by raising velocity of deformation to a power in order to make J a constant. This optimum power differed for each clay but all materials tested could be represented to the 0.18 power without excessive error.

Moisture content was then related to damping constant, J, for Veters clay. Liquidity index was related to J for all CH materials tested.

CHAPTER V

CONCLUSIONS

The conclusions drawn from this investigation are:

1. Based on applying the experimental laboratory data of this study to Smith's equation, Smith's J value varies with velocity of deformation for the materials tested.

2. Reeves' intercept method of modifying Smith's equation is valid only between loading velocities of 3-12 fps in sands and does not account for the initial portion of the load versus velocity of deformation curve.

3. Smith's equation can be modified to make J a constant for all values of load and velocity of deformation from 0-12 fps.

4. An acceptable constant J value for a clean sand may be obtained by raising velocity of deformation to the 0.20 power.

5. An acceptable constant J value for a highly plas-

tic clay may be obtained by raising velocity of deformation to the 0.18 power.

6. An approximate J value may be obtained:

- a. For a particular clean sand if its void ratio is known.

- b. For any clean sand if its effective angle of internal shearing resistance is known.

7. An approximate J value may be obtained:

- a. In a particular highly plastic clay if its moisture content is known.

- b. In any highly plastic clay if its liquidity index is known.

8. Other bands of data are believed to exist for materials other than clean sands and highly plastic clays based on tests performed on Hall Pit sandy clay.

CHAPTER VI

RECOMMENDATIONS

This investigation is a beginning in relating common properties of soils to a damping constant. Similar tests on other soils could shed light on J values for other materials such as silts and materials of low plasticity and could more specifically define the data obtained in this investigation. At the conclusion of a similar study, values of J could probably be approximated for most soils so that a more accurate analysis could be made by means of the wave equation application with the digital

computer. Thus a similar study is recommended covering:

1. Highly plastic clays and clean sands different from those involved in this investigation with the objective of further defining the relationships set forth in this study.

2. Various materials intermediate between clean sands and highly plastic clays with the objective of discovering relationships between J and similar or other soil properties.

References

1. Chan, Paul C., "A Study of Dynamic Load-Deformation and Damping Properties of Soils Concerned with a Pile Soil System," Ph.D. Dissertation, May 1967, Texas A&M University.
2. Hampton, D., and Yoder, E. J., "The Effect of Rate of Strain on Soil Strength," Proc. 44th Annual Road School, 1958, Purdue University.
3. Jones, R., Lister, N. W., and Thrower, E. N., "The Dynamic Behavior of Soils and Foundations," *Vibration in Civil Engineering*, Session IV, Proceedings of a Symposium organized by the British National of the International Society for Earthquake Engineering, London, April 1965.
4. Nishida, Yoshichika, "A Soil Strength Subject to Falling Impact," *Vibration in Civil Engineering*, Session IV, Proc. of a Symposium organized by the British National of the International Society for Earthquake Engineering, London, April 1965.
5. Reeves, Gary N., "Investigation of Sands Subjected to Dynamic Loading," Master of Science Thesis, December 1967, Texas A&M University.
6. Raba, Carl F., "The Static and Dynamic Response of a Miniature Friction Pile in Remolded Clay," Ph.D. Dissertation, January, 1968, Texas A&M University.
7. Samson, Charles H., Jr., "Pile-Driving Analysis by the Wave Equation (Computer Application)," Report of the Texas Transportation Institute, A&M College of Texas, May 1962.
8. Samson, C. H., Jr., Hirsch, T. J., and Lowery, L. L., "Computer Study of Dynamic Behavior of Piling," a paper presented to the Third Conference on Electronic Computation, ASCE, Boulder, Colorado, June 1963.
9. Shiffert, John B., "An Evaluation of the 'vac-aire' Extrusion Machine and an Investigation of Properties of Extruded Samples," Master of Science Thesis, January 1967, Texas A&M University.
10. Smith, E. A. L., "Pile Driving Analysis by the Wave Equation," *Transactions of ASCE*, Paper No. 3306, Vol. 127, Part I, 1962.
11. Sulaiman, I. H., "Skin Friction for Steel Piles in Sand," Master of Science Thesis, May 1967, Texas A&M University.
12. Whitman, R. V., and Healy, K. E., "Shearing Resistance of Sands During Rapid Loadings," *Transactions of ASCE*, Vol. 127, Part I, 1963.

Appendix A

DATA REDUCTION FROM THE VISICORDER TRACE

The Visicorder Trace

A sample visicorder trace is shown in Figure A-1. This trace was taken from a test performed on Victoria sand. The test was an unconsolidated-undrained test at a confining pressure of 15 psi and a void ratio of 0.55. The height of drop was 3.0 inches. The following discussion shows how velocity of deformation in feet per second and load in pounds were determined. On the left side of the trace in Figure A-1 is shown a calibration curve for the load. In going from A to B a load was placed on the load cell greater than that anticipated on the sample. This load was 1,000 pounds which deflected the visicorder point light source by 1.98 inches or 19.8 tenths of an inch. Tenths of an inch are used here since the visicorder paper is divided into tenths of an inch. Dividing 19.8 tenths of an inch into 1,000 pounds we arrive at a calibration factor of 50.5 pounds per tenth of an inch deflection.

By placing the linear displacement transducer in a device to deflect its shaft 0.1 inch we get a deflection or attenuation of the point light sources on the visicorder channel of 2.25 inches as shown going from C to D. With the calibration completed, the loads and deflections were again set to zero as seen in lines E and F of the trace. A saturated sand sample was then prepared for impact. For these tests the visicorder was run at a speed of 80 inches per second. It placed timing lines vertically on the photographic paper at intervals of 0.01 seconds. Points G and H represent the points of impact between the free falling weight and the sand sample.

At this point line HI begins to deflect downward from H to I indicating sample deformation and the load trace GJK begins to deflect upward indicating increase in load. Over the space of .00303 seconds the test has been completed: the sample deflection has gone off the paper and the load has returned to zero. Knowing the calibration factor the peak dynamic load at point J may be calculated by measuring the height in tenths of an inch to which load increased, then multiplying by 50.5 pounds per tenth of an inch deflection.

The velocity of sample deformation may be calculated from the deformation trace on the visicorder paper, which is really a deformation versus time curve. It is important to note that the deformation line is straight immediately after contact indicating constant velocity and zero acceleration. In order to calculate velocity, the deformation line must be divided into horizontal (time) and vertical (sample deformation) components. These components may be any size or may be taken at any point on the straight line since a proportion will result. The time interval may be calculated from this proportion:

$$\frac{\text{Horizontal displacement of event in inches}}{\text{Horizontal displacement of .01 sec. in inches}} = \frac{\text{unknown time}}{.01 \text{ sec.}}$$

$$\frac{.242 \text{ in.}}{.8 \text{ in.}} = \frac{\text{unknown time}}{.01 \text{ sec.}}$$

$$\text{unknown time} = .00303 \text{ sec.}$$

The vertical distance is the sample deformation in inches.

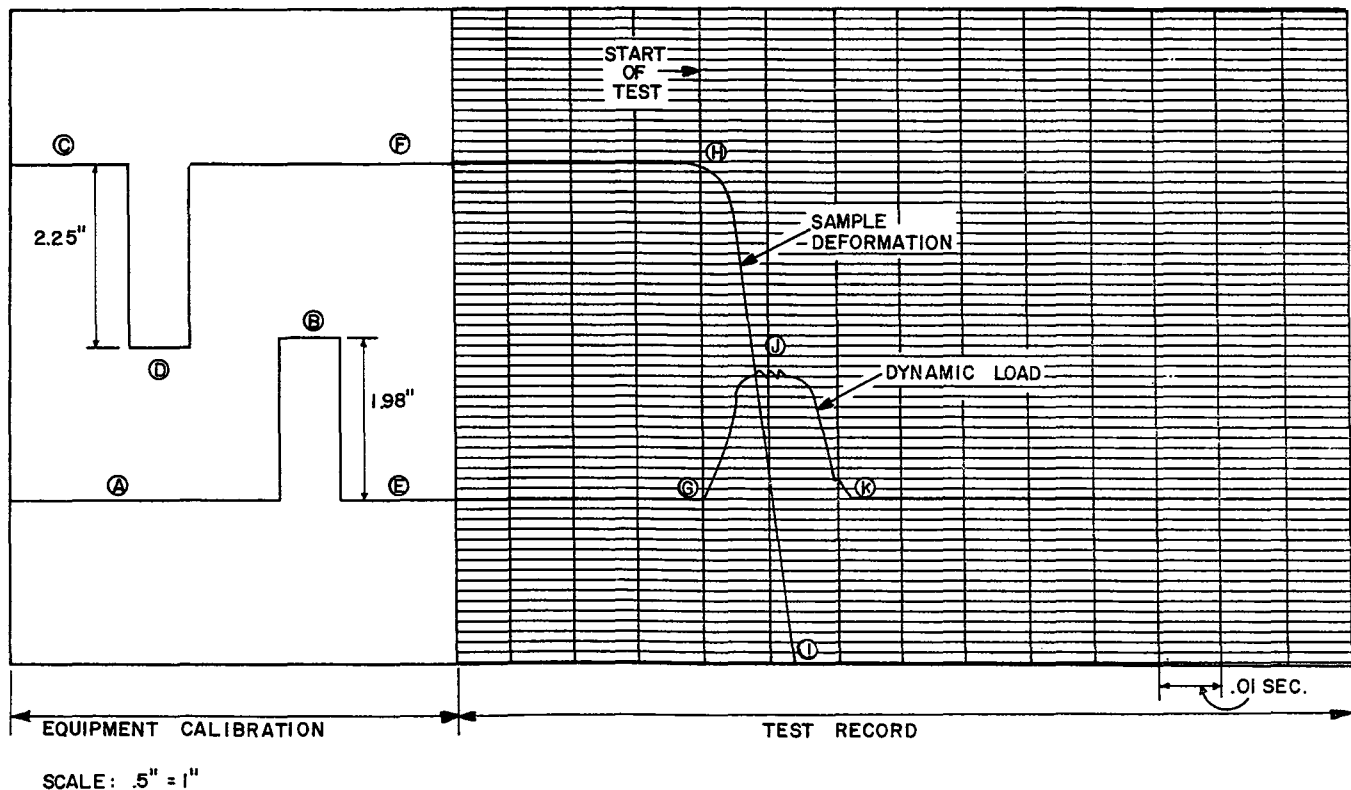


Figure A-1. Sample visicorder trace.

To obtain this deformation the vertical component is measured and then divided by the attenuation:

$$\begin{aligned} \text{Sample deformation} &= \frac{\text{Vertical length of component in inches}}{\frac{2.25 \text{ inches of deflection}}{.1 \text{ inch sample deformation}}} \\ &= \frac{6.2 \text{ inches}}{\frac{2.25 \text{ inches}}{.1 \text{ inch}}} \end{aligned}$$

$$\text{Sample deformation} = .2755 \text{ inches}$$

$$\begin{aligned} \text{Velocity of deformation} &= \frac{\text{sample deformation}}{\text{time length of event}} \\ &= \frac{.2755}{.00303} = 91 \text{ ips} \end{aligned}$$

dividing by 12 to get velocity in feet per second,

$$\text{Velocity of deformation} = 7.6 \text{ fps.}$$

Appendix B

EXPLANATION OF COMPUTER PROGRAM TO DETERMINE DAMPING CONSTANT

In modifying Smith's equation to determine a constant J, it was necessary to raise velocity of deformation to many different powers in order to arrive at an optimum power. To accomplish this, use was made of the IBM 360 Digital Computer. The program used to calculate the various J values is shown on pages 20-23. A flow diagram of this program is shown on page 24.

Use of the Computer Program

This program is made in sections, each section pertaining to a particular soil. For instance, in this investigation three sands were tested. Thus lines 2-14 (found on far left of program printout) represent Ottawa sand, 15-27 represent Arkansas sand and 28-40 represent Victoria sand. There must be one section for each soil or for each moisture content in the case of the cohesive materials. These sections are seen to be duplicates of one another with the following possible exceptions:

1. On lines 2, 15, 28, 41, 54, 67, 80, 93, 106, 119, 132, or the first card in each section is printed the number of data cards necessary for that particular soil. All data from one test will be put on one card.
2. The second card in each section indicates the lowest power to which velocity of deformation is to be raised. This should be a positive number to obey Smith's mathematical model.
3. In lines 8, 21, 34, 47, 60, 73, 86, 99, 112, 125, and 138 are seen the increments of the powers of velocity of deformation. In this case increments of 0.01 were used.
4. In lines 14, 27, 40, 53, 66, 79, 92, 105, 118, 131, and 144 are seen an "IF" statement which gives the highest power to which velocity may be raised. This

may be between the minimum described in step 2 and 1.0 which is Smith's power of velocity.

5. In lines 4, 7, 8, 9 and 13 for Ottawa sand are seen statement numbers. Statement numbers must not be duplicated if more sections are to be added to the program.

For this study the minimum power of velocity of deformation was 0.1 and the maximum was 0.36. Values of J were calculated for velocities of deformation in this range using an increment of 0.01.

One data card is required for each test performed. The information on each data card pertains to that particular test. Sample data are shown printed at the end of the program on page 77. The numbers in the following discussion which are referred to as decimal numbers should not exceed 10 digits total and should have no more than three digits to the right of the decimal point. The following input format is used for each data card:

1. In spaces 1-9 on the data card is printed any combination of numbers or letters describing the soil tested. This is a non-decimal number.
2. In spaces 10-19 on the data card is printed the number of the test which should be oriented to the right of the spaces allotted if it does not completely fill the space. This is a non-decimal number.
3. In spaces 20-29 on the card are printed velocity of deformation which is a decimal number.
4. In spaces 30-39 on the card is printed the height of drop which is a decimal number.
5. In spaces 40-49 on the card is printed the peak dynamic load in pounds which is a decimal number.
6. In spaces 50-59 on the card is printed the static load for the material which is a decimal number.

\$JOB 482G6,TIME=001,PAGES=100 GIBSON THESIS

\$IRBOX 08-J

1 DIMENSION VEL(25),DROP(25),PDYN(25),PSTA(25),PRA(25),PJ(25),
IITEST(25)

C
C THIS PROGRAM IS TO DETERMINE VALUES FOR DAMPING COEFFICIENTS IN
C SOILS

C
C OTTA IS OTTAWA SAND TESTED SATURATED UNDRAINED

C
2 N=21
3 XN=0.1
4 DO 1 J=1,N
5 READ(5,101) NAME,IITEST(J),VEL(J),DROP(J),PDYN(J),PSTA(J)
6 WRITE(6,31) NAME,IITEST(J),VEL(J),DROP(J),PDYN(J),PSTA(J),XN
7 1 CONTINUE
8 51 XN=XN+0.01
9 DO 8 I=1,N
10 PRA(I)=PDYN(I)/PSTA(I)
11 PJ(I)=(1.0/(VEL(I)**XN)*(PRA(I)-1.0))
12 WRITE(6,21) I,PJ(I),XN,IITEST(I),NAME
13 8 CONTINUE
14 IF(XN-0.35) 51,63,63

C
C ARKA IS ARKANSAS SAND TESTED SATURATED UNDRAINED

15 63 N=18
16 XN=0.1
17 DO 3 J=1,N
18 READ(5,101) NAME,IITEST(J),VEL(J),DROP(J),PDYN(J),PSTA(J)
19 WRITE(6,31) NAME,IITEST(J),VEL(J),DROP(J),PDYN(J),PSTA(J),XN
20 3 CONTINUE
21 52 XN=XN+0.01
22 DO 4 I=1,N
23 PRA(I)=PDYN(I)/PSTA(I)
24 PJ(I)=(1.0/(VEL(I)**XN)*(PRA(I)-1.0))
25 WRITE(6,21) I,PJ(I),XN,IITEST(I),NAME
26 4 CONTINUE
27 IF(XN-0.35) 52,64,64

C
C VICT IS VICTORIA SAND TESTED SATURATED UNDRAINED

28 64 N=12
29 XN=0.1
30 DO 5 J=1,N
31 READ(5,101) NAME,IITEST(J),VEL(J),DROP(J),PDYN(J),PSTA(J)
32 WRITE(6,31) NAME,IITEST(J),VEL(J),DROP(J),PDYN(J),PSTA(J),XN
33 5 CONTINUE
34 53 XN=XN+0.01
35 DO 6 I=1,N
36 PRA(I)=PDYN(I)/PSTA(I)
37 PJ(I)=(1.0/(VEL(I)**XN)*(PRA(I)-1.0))
38 WRITE(6,21) I,PJ(I),XN,IITEST(I),NAME
39 6 CONTINUE
40 IF(XN-0.35) 53,65,65

C
C OR35 IS AN ORGANIC MATERIAL WITH A THIRTY FIVE PERCENT MOISTURE
C CONTENT

41 65 N=17
42 XN=0.1
43 DO 7 J=1,N
44 READ(5,101) NAME,IITEST(J),VEL(J),DROP(J),PDYN(J),PSTA(J)
45 WRITE(6,31) NAME,IITEST(J),VEL(J),DROP(J),PDYN(J),PSTA(J),XN
46 7 CONTINUE
47 54 XN=XN+0.01
48 DO 10 I=1,N
49 PRA(I)=PDYN(I)/PSTA(I)
50 PJ(I)=(1.0/(VEL(I)**XN)*(PRA(I)-1.0))
51 WRITE(6,21) I,PJ(I),XN,IITEST(I),NAME

```

52      10 CONTINUE
53      IF(XN-0.35) 54,66,66
      C
      C      EA60 IS FOR EASTERWOOD SHALE WITH A SIXTY PERCENT MOISTURE
      C      CONTENT
54      66 N=14
55      XN=0.1
56      DO 9 J=1,N
57      READ(5,101) NAME,ITEST(J),VEL(J),DROP(J),PDYN(J),PSTA(J)
58      WRITE(6,31) NAME,ITEST(J),VEL(J),DROP(J),PDYN(J),PSTA(J),XN
59      9 CONTINUE
60      55 XN=XN+0.01
61      DO 2 I=1,N
62      PRA(I)=PDYN(I)/PSTA(I)
63      PJ(I)=(1.0/(VEL(I)**XN)*(PRA(I)-1.0))
64      WRITE(6,21) I,PJ(I),XN,ITEST(I),NAME
65      2 CONTINUE
66      IF(XN-0.35) 55,67,67
      C
      C      EA55 IS FOR EASTERWOOD CLAY WITH A MOISTURE CONTENT OF
      C      FIFTY FIVE PERCENT
67      67 N=9
68      XN=0.1
69      DO 11 J=1,N
70      READ(5,101) NAME,ITEST(J),VEL(J),DROP(J),PDYN(J),PSTA(J)
71      WRITE(6,31) NAME,ITEST(J),VEL(J),DROP(J),PDYN(J),PSTA(J),XN
72      11 CONTINUE
73      56 XN=XN+0.01
74      DO 12 I=1,N
75      PRA(I)=PDYN(I)/PSTA(I)
76      PJ(I)=(1.0/(VEL(I)**XN)*(PRA(I)-1.0))
77      WRITE(6,21) I,PJ(I),XN,ITEST(I),NAME
78      12 CONTINUE
79      IF(XN-0.35) 56,68,68
      C
      C      EA50 IS FOR EASTERWOOD CLAY WITH A MOISTURE CONTENT OF
      C      FIFTY PERCENT
80      68 N=6
81      XN=0.1
82      DO 13 J=1,N
83      READ(5,101) NAME,ITEST(J),VEL(J),DROP(J),PDYN(J),PSTA(J)
84      WRITE(6,31) NAME,ITEST(J),VEL(J),DROP(J),PDYN(J),PSTA(J),XN
85      13 CONTINUE
86      57 XN=XN+0.01
87      DO 14 I=1,N
88      PRA(I)=PDYN(I)/PSTA(I)
89      PJ(I)=(1.0/(VEL(I)**XN)*(PRA(I)-1.0))
90      WRITE(6,21) I,PJ(I),XN,ITEST(I),NAME
91      14 CONTINUE
92      IF(XN-0.35) 57,69,69
      C
      C      VE55 IS FOR VETTERS CLAY WITH A MOISTURE CONTENT OF
      C      FIFTY FIVE PERCENT
93      69 N=13
94      XN=0.1
95      DO 15 J=1,N
96      READ(5,101) NAME,ITEST(J),VEL(J),DROP(J),PDYN(J),PSTA(J)
97      WRITE(6,31) NAME,ITEST(J),VEL(J),DROP(J),PDYN(J),PSTA(J),XN
98      15 CONTINUE
99      58 XN=XN+0.01
100     DO 16 I=1,N
101     PRA(I)=PDYN(I)/PSTA(I)
102     PJ(I)=(1.0/(VEL(I)**XN)*(PRA(I)-1.0))
103     WRITE(6,21) I,PJ(I),XN,ITEST(I),NAME
104     16 CONTINUE
105     IF(XN-0.35) 58,70,70
      C
      C      VE50 IS FOR VETTERS CLAY WITH A MOISTURE CONTENT OF

```

```

C      FIFTY PERCENT
C
106    70 N=14
107      XN=0.1
108      DO 17 J=1,N
109      READ(5,101) NAME,ITEST(J),VEL(J),DROP(J),PDYN(J),PSTA(J)
110      WRITE(6,31) NAME,ITEST(J),VEL(J),DROP(J),PDYN(J),PSTA(J),XN
111    17 CONTINUE
112    59 XN=XN+0.01
113      DO 18 I=1,N
114      PRA(I)=PDYN(I)/PSTA(I)
115      PJ(I)=(1.0/(VEL(I)**XN))*(PRA(I)-1.0))
116      WRITE(6,21) I,PJ(I),XN,ITEST(I),NAME
117    18 CONTINUE
118      IF(XN-0.35) 59,71,71
C      VE46 IS FOR VETTERS CLAY WITH A MOISTURE CONTENT OF
C      FORTY SIX PERCENT
119    71 N=13
120      XN=0.1
121      DO 19 J=1,N
122      READ(5,101) NAME,ITEST(J),VEL(J),DROP(J),PDYN(J),PSTA(J)
123      WRITE(6,31) NAME,ITEST(J),VEL(J),DROP(J),PDYN(J),PSTA(J),XN
124    19 CONTINUE
125    60 XN=XN+0.01
126      DO 20 I=1,N
127      PRA(I)=PDYN(I)/PSTA(I)
128      PJ(I)=(1.0/(VEL(I)**XN))*(PRA(I)-1.0))
129      WRITE(6,21) I,PJ(I),XN,ITEST(I),NAME
130    20 CONTINUE
131      IF(XN-0.35) 60,72,72
C      CE35 IS FOR CENTERVILLE SAND WITH A MOISTURE CONTENT OF
C      THIRTY FIVE PERCENT
C
132    72 N=13
133      XN=0.1
134      DO 23 J=1,N
135      READ(5,101) NAME,ITEST(J),VEL(J),DROP(J),PDYN(J),PSTA(J)
136      WRITE(6,31) NAME,ITEST(J),VEL(J),DROP(J),PDYN(J),PSTA(J),XN
137    23 CONTINUE
138    61 XN=XN+0.01
139      DO 22 I=1,N
140      PRA(I)=PDYN(I)/PSTA(I)
141      PJ(I)=(1.0/(VEL(I)**XN))*(PRA(I)-1.0))
142      WRITE(6,21) I,PJ(I),XN,ITEST(I),NAME
143    22 CONTINUE
144      IF(XN-0.35) 61,73,73
145      21 FORMAT(10X,I4,10X,F10.3,10X,F10.3,10X,I4,10X,A4)
146      31 FORMAT(A4,5X,I3,6X,F8.5,2X,F8.5,3X,F7.3,3X,F7.3,3X,F6.4)
147      101 FORMAT(A4,5X,I3,6X,F8.5,2X,F8.5,3X,F7.3,3X,F7.3)
148      73 CONTINUE
149    102 STOP
150      END

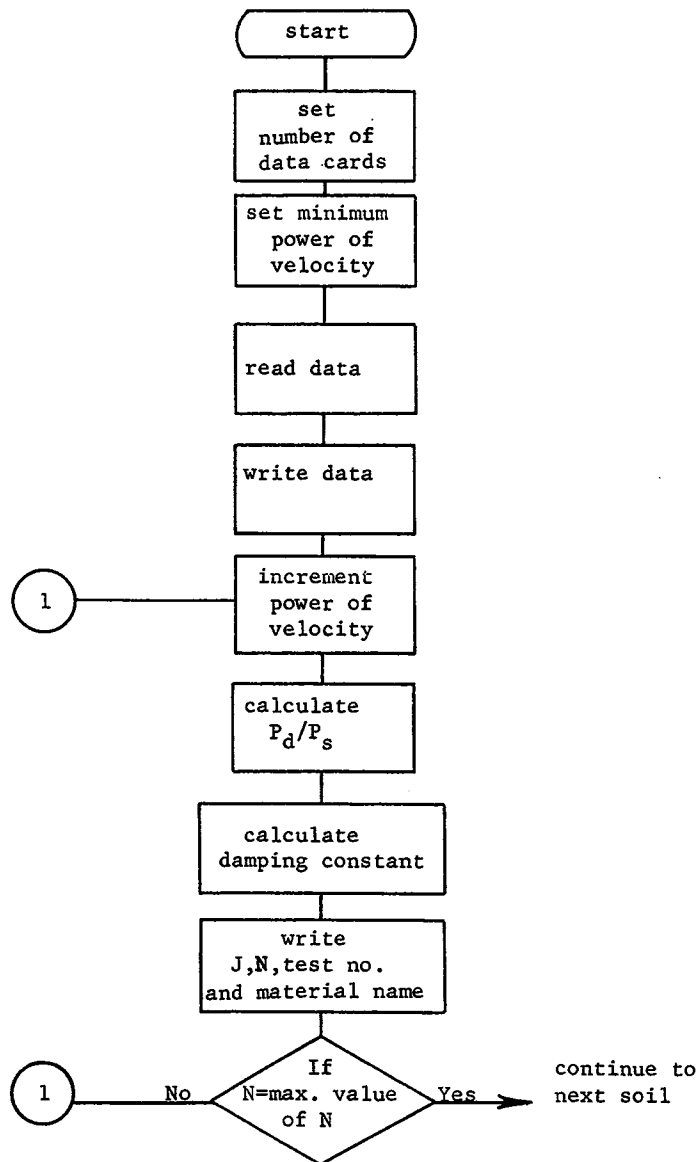
```

SAMPLE DATA

MATERIAL	TEST NO.	VELOCITY OF DEFORMATION	HEIGHT OF DROP	DYNAMIC LOAD	STATIC LOAD
EA50	115	0.99700	0.00000	125.000	63.500
EA50	114	2.90000	1.00000	134.500	63.500
EA50	113	4.40000	2.00000	136.400	63.500
EA50	112	5.48000	3.00000	144.000	63.500
EA50	111	9.04000	9.00000	154.500	63.500
EA50	110	10.31999	12.00000	156.000	63.500

ITERATION NUMBER	J-VALUE	N	TEST NO.	MATERIAL
6	1.051	0.140	110	EA50
1	0.969	0.150	115	EA50
2	0.953	0.150	114	EA50
3	0.919	0.150	113	EA50
4	0.982	0.150	112	EA50
5	1.030	0.150	111	EA50
6	1.026	0.150	110	EA50
1	0.969	0.160	115	EA50
2	0.943	0.160	114	EA50
3	0.906	0.160	113	EA50
4	0.966	0.160	112	EA50
5	1.008	0.160	111	EA50
6	1.003	0.160	110	EA50
1	0.969	0.170	115	EA50
2	0.933	0.170	114	EA50
3	0.892	0.170	113	EA50
4	0.949	0.170	112	EA50
5	0.986	0.170	111	EA50
6	0.980	0.170	110	EA50
1	0.969	0.180	115	EA50
2	0.923	0.180	114	EA50
3	0.879	0.180	113	EA50
4	0.933	0.180	112	EA50
5	0.964	0.180	111	EA50
6	0.957	0.180	110	EA50
1	0.969	0.190	115	EA50
2	0.913	0.190	114	EA50
3	0.866	0.190	113	EA50
4	0.918	0.190	112	EA50
5	0.943	0.190	111	EA50
6	0.935	0.190	110	EA50

FLOW DIAGRAM



Appendix C

DETERMINATION OF THE OPTIMUM POWER OF VELOCITY OF DEFORMATION

Once the computer analysis is complete it still remains to select the optimum power of velocity of deformation. This is accomplished graphically, the optimum power being the one yielding the least scatter in J values. Figure C-1 shows how the velocity of deformation may vary when raised to powers other than the optimum power. The bottom curve of this figure shows points calculated from Smith's original equation using EA 50 material as an example. Velocity of deformation is then shown raised to the 0.11 and 0.36 powers which are below and above the optimum power respectively. The optimum power of 0.19 for EA 50 material is shown as a horizontal line along with the optimum J value for this power. The sample output for the computer program shown on page 78 gives the data for the $N = 0.19$ curve represented in Figure C-1.

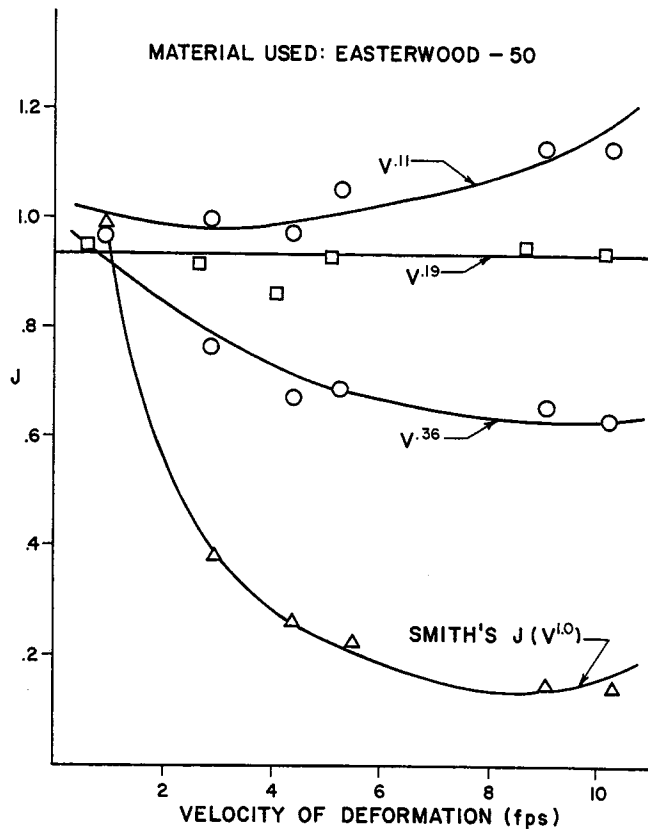


Figure C-1. Method of obtaining velocity to optimum power.

Appendix D

MOHR'S CIRCLE DIAGRAMS FOR THE GRANULAR MATERIALS TESTED

Explanation of the diagram

Mohr's circle diagrams are presented for the granular materials tested in Figures D-1, D-2, and D-3. These tests were all performed at a 0.55 void ratio. The confining pressures were varied as well as the conditions of

drainage. The drained tests were consolidated-drained tests and the undrained tests were unconsolidated-undrained tests with pore pressure measurements. The conditions involved in each test are indicated on Figures D-1, D-2, and D-3.

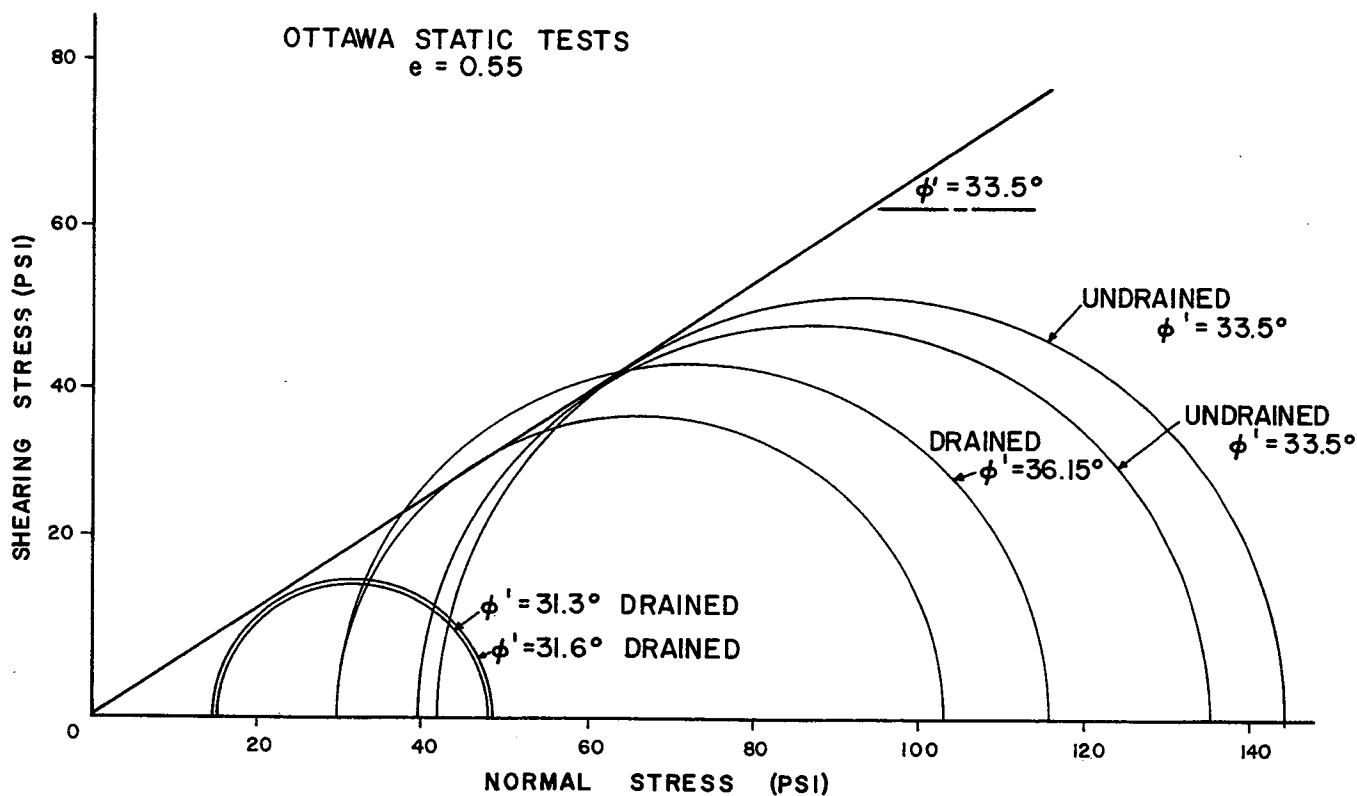


Figure D-1. Mohr's circle diagram for Ottawa sand.

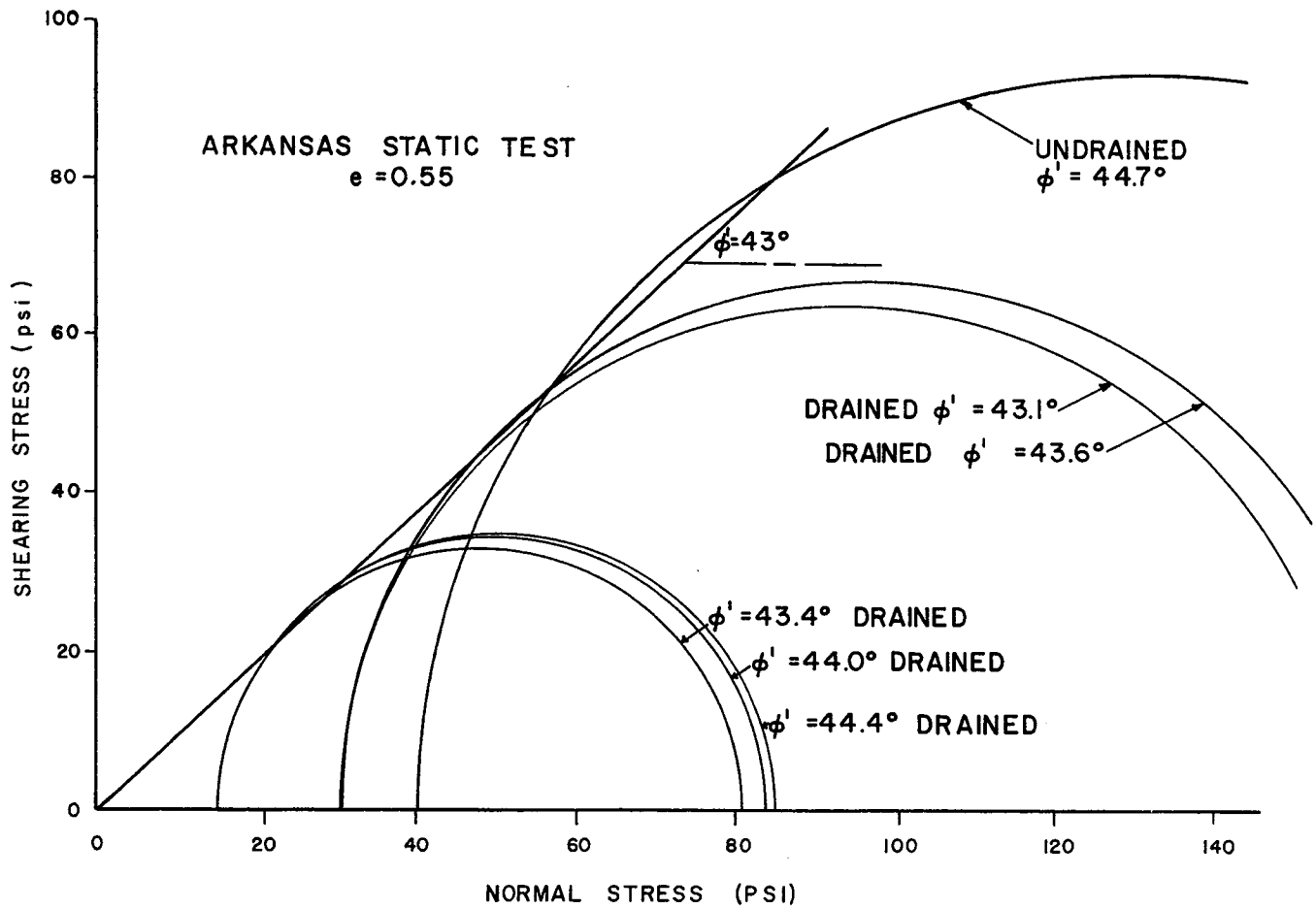


Figure D-2. Mohr's circle diagram for Arkansas sand.

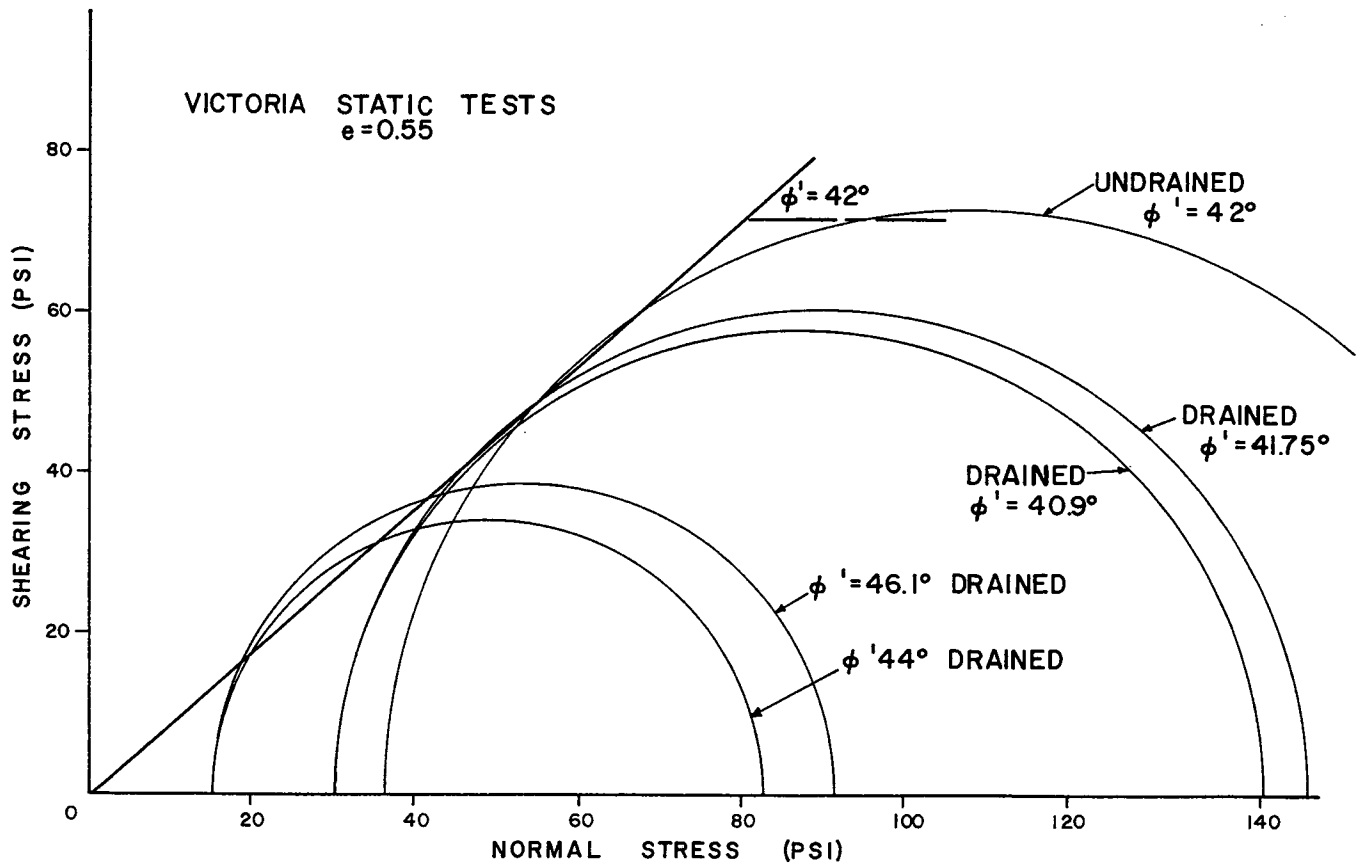


Figure D-3. Mohr's circle diagram for Victoria sand.

